Attributing and Verifying European and National Greenhouse Gas and Aerosol Emissions and Reconciliation with Statistical Bottom-up Estimates

Deliverable 4.1
Modelled C and N_2O fluxes and emission factors

Authors: Anna Maria Jönsson, Angela Fiore, Fredrik Lagergren, Tanya Lippmann, Mattias Lundblad, Kim Naudts, Hans Petersson, Yanzi Yan, Lorella Mariani, Eleonora Di Cristofaro

Date: 19/12/2025
Dissemination: Public
Work package: 4.1
Version: [1.0]

Funded by the European Union

This project has received funding from the European Union's Horizon Europe research and innovation programme under grant agreement No. 101081322

Attributing and Verifying European and National Greenhouse Gas and Aerosol Emissions and Reconciliation with Statistical Bottom-up Estimates (AVENGERS)

Call: HORIZON-CL5-2022-D1-02

Topic: HORIZON-CL5-2022-D1-02-01

Type of action: HORIZON Research and Innovation Actions

Granting authority: European Climate, Infrastructure and Environment Executive Agency

Project starting date: 01/01/2023

Project end date: 30/06/2026

Project duration: 42 months

Contact: Dr. Marko Scholze, Coordinator

Lund University, Sweden

Document history:

Version	Author(s)	Date	Changes
1.0	All	2025-12-19	Initial version

Internal review: ULUND project office, 2025-12-10

Table of Contents

1 Executive summary

The aim of Task 4.1 is to derive emission factors based on bottom-up land surface modelling, using two process-based dynamic global vegetation models (DGVMs), LPJ-GUESS and ORCHIDEE. In recent years, emission factors have been proposed as a useful methodology for estimating greenhouse gas emissions under different land-management strategies. Whilst emission factors are straightforward to implement and offer several practical advantages, conventional emission factors do not account for climatic variability (e.g., increased runoff following heavy precipitation in a wet year may reduce N_2O emissions) or spatial heterogeneity (differences in soil properties also impact CO_2 and N_2O emissions). To investigate the extent to which incorporating spatially and temporally explicit processes improves the robustness of GHG emission estimates, we assess the added value of representing spatial and temporal variability associated with land management and extreme weather events using two case studies: carbon emissions from forestry in Sweden and nitrogen emissions from agriculture in Italy. Model simulations were evaluated against available observational data. The simulations demonstrated the usefulness of DGVMs for estimating spatial and temporal changes in carbon stock (forest in Sweden) and N_2O emissions (agriculture in Italy), as influenced by weather and climate extremes and different management methods. The model comparison revealed that uncertainties in model parameterization can significantly affect simulation outcome, highlighting the need for further model development, calibration, and evaluation.

2 Estimation of C and N fluxes for the AFOLU sector from terrestrial ecosystem models

The objective of task 4.1 was to derive emission factors based on bottom-up land surface modelling, using two process-based dynamic global vegetation models (DGVMs): LPJ-GUESS and ORCHIDEE. Task 4.1 included two case studies (link to WP1), forest in Sweden and agriculture in Italy, with process attribution of GHG emissions to improve the spatial and temporal resolution and enable assessments of management decisions and extreme weather events.

The aim was to compare model estimates to national inventory reporting and IPCC emission factors in order to 1) provide country and county specific estimates on stock-change based carbon emissions (forest in Sweden) and N_2O emissions (agriculture in Italy), 2) account for temporal patterns such as annual variability induced by impacts of weather and climate extremes, 3) estimate the impact of different management methods, and 4) provide model uncertainty assessments.

2.1 LPJ-GUESS

The LPJ-GUESS model provides a process-based representation of ecosystem function and vegetation structure (Smith et al., 2001, 2014). The basic level of a simulation is a forest patch in which cohorts of different plant functional types (PFTs) compete for light, nitrogen, and water, resulting in a net primary production (NPP) that is allocated to new biomass of the cohort. Establishment of new cohorts is regulated by potential NPP at the forest floor and PFT related parameters. Mortality related to competition and age is simulated annually and patch-destroying disturbances at a fixed interval (300 years in the presented simulations). Cohort NPP and water dynamics are simulated daily, driven by precipitation, temperature and radiation data. PFTs exist both in a generic global set and a European set (Hickler et al. 2012), which includes most tree species found in Sweden.

Forest management (Lagergren et al. 2012, Lindeskog et al. 2023) is simulated for groups of patches, called a stand type, where specifications of species planted, thinning regime and rotation period determines harvest and establishment, replacing natural disturbances. Storm and spruce bark beetle damage is explicitly simulated (Lagergren et al. 2012, Jönsson et al. 2012, Lagergren et al. 2025). The land-use functionality also includes setting for cropland and grassland, with a special set of PFTs, for which detailed information of fertilization, irrigation, sowing dates and tillage can be specified (Olin et al. 2015).

2.2 ORCHIDEE

ORCHIDEE (Organising Carbon and Hydrology In Dynamic Ecosystems) is developed (primarily) at the IPSL (Institut Pierre Simon Laplace). ORCHIDEE is designed to simulate carbon, nitrogen, water, and energy fluxes from local sites to the global level (Krinner et al. 2005, Vuichard et al 2019). It calculates the energy and hydrology budget of the terrestrial biosphere at half-hourly intervals. ORCHIDEE typically distinguishes 15 plant functional types. However, the number of PFTs can vary depending on the model’s application. ORCHIDEE simulates vegetation phenology and carbon dynamics, including photosynthesis, maintenance and growth respiration, within plant carbon and nitrogen allocation, plant mortality, production and decomposition of litter, and soil carbon and nitrogen dynamics, at daily time steps. Mortality can be caused by “background mortality” and as a result of natural disturbances, i.e., fire, wind and bark beetles, and anthropogenic disturbances, i.e. land cover changes and forest management.

ORCHIDEE is forced with meteorological data, atmospheric CO_2 concentration, a river network map, a forest management map, nitrogen input maps of fertilisation and atmospheric deposition, a soil texture map, and land cover maps to prescribe the vegetation distribution. The vegetation distribution is represented by the areal proportion of each PFT in each model grid cell for a given point in time. When land cover changes happen, PFT-level carbon stocks are redistributed from the shrinking PFT to the expanding one.

To represent forest stand structure, ORCHIDEE uses, typically three, diameter classes (Naudts et al 2015, Bellassen et al. 2010). In the case of even-aged stands, all diameter classes are equal. As trees within the stand grow, relative density increases. Different management strategies are assigned a target of relative density. In the case that the stand is on the verge of overstocking, the target of relative density has been reached, and self-thinning occurs. The stand is harvested if thinning would result in unrealistically low stand density or unrealistically large diameters of the remaining trees. In the case of unmanaged forests, overstocking results in self-thinning. Different management strategies have different targets for relative density and cut different diameter classes. In the historical simulations ORCHIDEE was configured to simulate even-aged rotational management or unmanaged forests. For the future simulations also a conversion to continuous cover forestry after a stand replacing disturbance, was tested.

ORCHIDEE simulates typical forestry variables such as basal area, stand density, quadratic mean diameter, quadratic mean height and diameter distribution. The carbon and nitrogen balance of the forest is represented by: (i) the net change of carbon and nitrogen pools in forest ecosystems; (ii) the carbon stored in the short, medium and long-lived harvested wood, which act as ex-situ carbon sinks.

The nitrogen cycle is represented at the PFT level as for the carbon cycle, and for each carbon pool there is a corresponding nitrogen pool, with C/N ratios evolving through time (Vuichard et al., 2019). The leaf C/N ratio is dynamic and varies according to nitrogen supplied by the roots and demand for biomass allocation. The fate of mineral nitrogen in the soil follows the same formalism of processes as the OCN model (Zaehle and Friend, 2010a, Zaehle and Friend, 2010b). Nitrogen inputs in the soil–plant system are related to (i) atmospheric nitrogen deposition in the form of NH_x and NO_y components, (ii) biological nitrogen fixation (BNF) on any land category, and (iii) nitrogen fertilisation over managed grasslands and croplands.

2.3 Model input data: climate, CO_2, nitrogen deposition and soil

To drive the model simulations, 6-hour meteorological data were obtained from the CRU JRA v2.4 forcing dataset (https://catalogue.ceda.ac.uk/uuid/aed8e269513f446fb1b5d2512bb387ad) and aggregated to daily values, for 1901-2022 with a spatial resolution of 0.5° × 0.5°.

For CO_2 concentration we used annual data from the Global Carbon Project (Le Quéré et al., 2018). For LPJ-GUESS, monthly values at 10-year intervals, based on Lamarque et al. (2011), were used as nitrogen deposition input data, and soil data were taken from the ISRICE-WISE global data set (Batjes 2005). For ORCHIDEE, atmospheric N deposition (NHx-N and NOy-N) was from the International Global Atmospheric Chemistry (IGAC)/Stratospheric Processes and Their Role in Climate (SPARC) Chemistry–Climate Model Initiative (CCMI) N deposition fields (Tian et al. 2018). The fraction of agricultural land that is irrigated is based on Siebert et al. (2005) initially available at 5 arc-min.

2.4 Forest simulation strategy and output data

The two DGVMs ORCHIDEE and LPJ-GUESS were applied to simulate current forest conditions (incl. carbon stock development), soil carbon dynamics, and forest management for Sweden.

2.4.1 LPJ-GUESS model setup

For the Swedish case a version of LPJ-GUESS with the most recent developments of forest-management input, detailed output options and an update of parameters for the European PFTs was used (LPJ-GEUSS v4.1, european_applications branch, revision 13145). For potential natural vegetation, the average return time for generic patch-destroying disturbances was set to 300 years, but this was turned off in managed stands. In managed stands, wind damage was driven by a wind-load file (Lagergren et al. 2012) based on observed wind damage 1961-2010 (Marini et al., 2017) and CRU JRA wind data for the remaining historical years. Spruce bark beetle damage was simulated (Lagergren et al. 2025) using temperature, drought and storm damaged spruce as drivers.

National Forest Inventory (NFI) data for the period 1988-1992 were used to initialize forest conditions, with county-level data on seven forest types (*Pinus sylvestris* pine forest, *Pinus contorta* pine forest, Spruce forest, mixed needle-leaf forest, mixed forest dominated by broad-leaf species, nemoral broadleaf forest, and boreal broadleaf forest) and twelve age-classes (0-2, 3-10, 11-20, 21-30, 31-40, 41-60, 61-80, 81-100, 101-120, 121-140, 141-160, and 161+ years).

The forest type and age distribution data were translated into six species types with 10-year age classes, continuous forestry and unmanaged forest, managed with different rotation periods for different parts of the country (Figure 1). Details of the simulation strategy for the Sweden forest case study are provided in Annex 1.

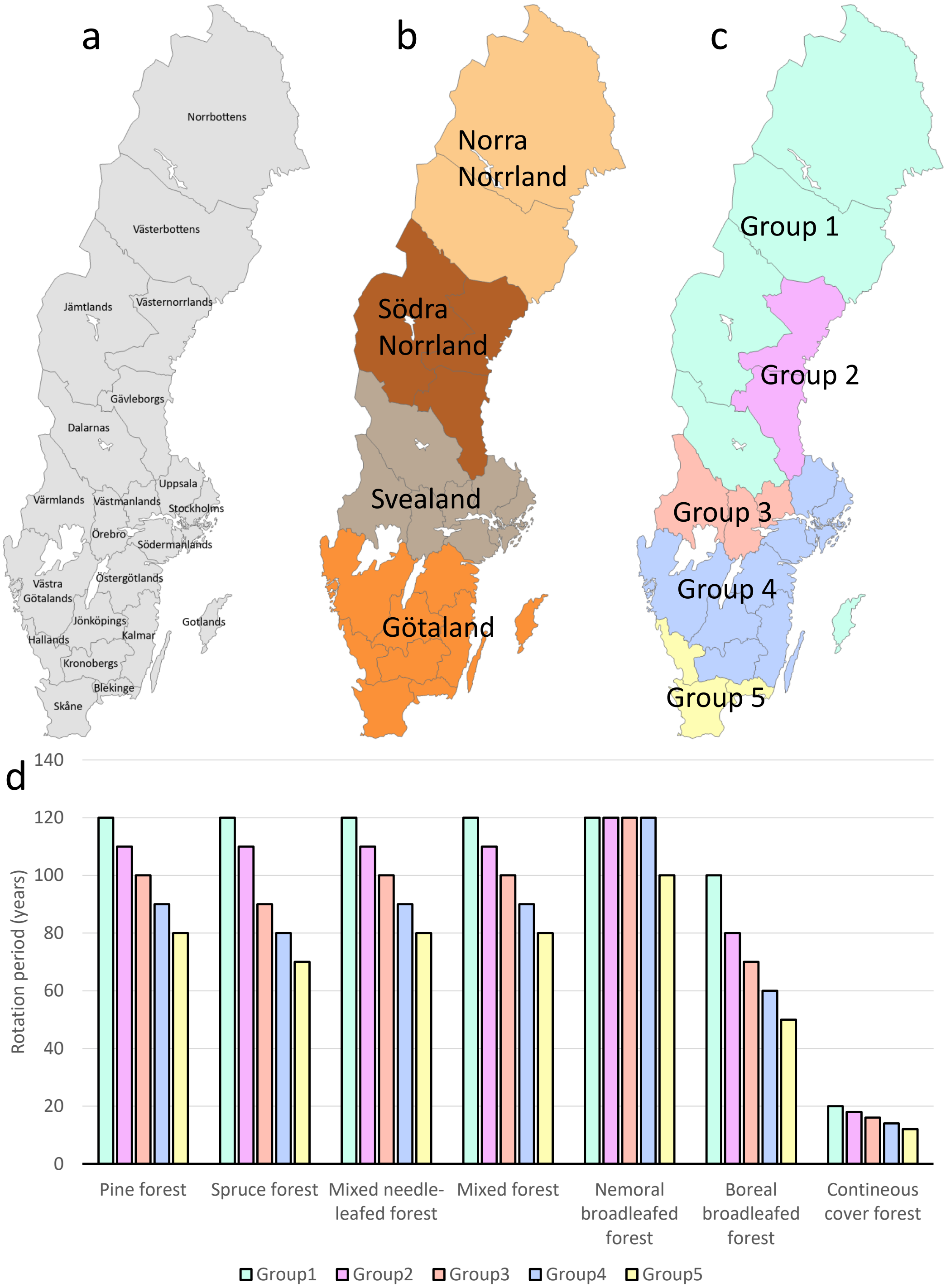

Figure 1. The counties in Sweden (a), the traditional division into country parts (b), the division used in LPJ-GUESS to group regions with the same rotation periods (c), and the rotation periods for the LPJ-GUESS groups (d). Note that the island of Gotland has a dry climate and coarse, shallow soil which make it part of the northern Group 1. For continuous cover forest, the return time of cuttings is given instead of rotation period.

2.4.2 ORCHIDEE model setup

For ORCHIDEE, the simulation experiment consists of: (1) a 600-year model spinup, (2) the construction of a 200-year lookup-table, (3) nudging of the initial conditions for 1990, (4) a 35-year historical simulation from 1990 to 2025. All simulation components were run at 0.5 x 0.5 degrees resolution. After the soil pools have reach equilibrium (i.e. year 400 of spinup simulation), all forests are clear-cut and the simulation is extended for a final 200 years to generate the lookup table. This process is to ensure that the simulation over the historical period begins with soils that are in equilibrium and a realistic representation of forest composition.

Spinup

The spinup was run by recycling 1971-1990 climate data for 400 years to allow the soil nitrogen and carbon pools to reach equilibrium. During the spinup, the atmospheric CO_2 concentration was constant (350ppm). The model was configured to simulate the following 8 forest PFTs in Sweden: Temperate Needleleaf Evergreen, Temperate Picea Sp, Temperate Broad Leaved Summergreen, Boreal Needleleaf Evergreen, Boreal Picea Sp, Boreal Broad Leaved Summergreen, Boreal Larix Sp. All PFTs were simulated with a single age class and three diameter classes.

Constructing the lookup table to nudge the initial conditions

Following the clear cut all PFTs are replanted and the vegetation is managed according to the forest management map for the year 2020. The forest management map combined ORCHIDEE specific 17PFT (2023.v1) maps (derived from ESACCI LC v2.0.82) with the LUHv2 division (Hurtt et al. 2020) between primary and secondary forest to obtain a historical record of ORCHIDEE specific forest management maps. If the stand is managed, a proportion of the biomass is harvested and put into wood product pools. If, however, the stand is unmanaged, the biomass remains on site. Results from the 200 year regrowth simulation are then used to compile the look up table which consists of a diameter for each PFT, for each grid cell. For each grid cell and PFT, the simulated mean diameter (including all related prognostic variables used within ORCHIDEE) from the 200 years of the regrowth simulation that is closest to the observed mean diameter (for that PFT and grid cell) is selected.

An observational tree diameter map, re-gridded to 0.5° x 0.5°, was used to construct the present-day forest conditions (Pucher et al 2022). The Pucher map contains data from the period between 2000 and 2010 and was therefore assumed to represent the year 2005. The WP simulation protocol required the simulation to start in 1990. Therefore, instead of using the year associated with the diameter closest to the observation, the lookup table used simulated carbon, nitrogen, water and energy pools from 15 years earlier to compile the restart file.

Future model simulations

To compare different forest management strategies, we continued the historical model simulation for the period 2020 – 2100 using ssp370 climate scenario as a future climate forcing (ISIMIP, https://data.isimip.org) (Frieler et al 2024). We ran three future simulations each with a different forest management strategy: unmanaged, high stand management, and continuous cover forestry. Beginning from the historical run which used the 2020 forest management map described above, the management was gradually changed to either unmanaged, high stand management, or continuous cover forestry after a stand replacing disturbance occurred. Note that historically unmanaged forest remained unmanaged.

2.4.3 Compilation of model results and comparison to inventory-based data

Mean carbon fluxes (ton C ha^{-1} yr^{-1}) and pools (ton C ha^{-1}) across all simulated forest area are provided at grid-cell and county level and also summed up to country totals. The simulated total net emissions were compared with the inventory-based numbers reported to UNFCCC. The net change in carbon pools was also calculated and compared to Sweden's reported numbers. The net ecosystem exchange and the net change in vegetation carbon pool were assessed for the different simulated species types, continuous forestry, and unmanaged forest by county to explore the potential impact of alternative forest management strategies. To limit the number of figures presented, some results were shown for the four traditional country parts (Figure 1). For verification of the model, the results were compared to county level NFI data in 2020 (2018-2022 inventory) of tree biomass and mean tree diameter.

Model results of carbon emissions from different pools were compared with reported values based on NFI data at the country scale to address uncertainties and knowledge gaps in estimating emissions for the simulation period 1991-2020. The impact of extreme climate events (summer drought in 2018) was analysed. The simulations were further analysed to indicate the potential impact of alternative forest management strategies, comparing different species types of even-age forestry (EAF) and continuous cover forestry (CCF).

2.4.4 LPJ-GUESS output data:

Raw ASCII-format output files, ncdf-files of key variables compiled to 0.5° grid or to counties, and files for the setup of the simulations are stored at ICOS Carbon Portal fileshare (https://fileshare.icos-cp.eu/apps/files/files/4880159?dir=/AVENGERS/WP4-Process_modelling/Tasks/Task%204.1%20documentation/Model%20output%20data/LPJGUESS/SwedenCaseStudy). Further details are given in the ReadMe file of the directory.

2.4.5 ORCHIDEE output data:

The model results are stored as ncdf-files divided in vegetation and soil carbon output (SBG, stomate*.nc) and energy and water budget output (SRF, sechiba*.nc) at ICOS Carbon Portal fileshare (https://fileshare.icos-cp.eu/apps/files/files/4867313?dir=/AVENGERS/WP4-Process_modelling/Tasks/Task%204.1%20documentation/Model%20output%20data/ORCHIDEE). Further details are given in the ReadMe file of the directory.

2.5 Agriculture simulation strategy and output data

For the purpose of the AVENGERS project, we are focusing our attention on the following Italian GHG Inventory estimate: direct N_2O emissions and indirect (from volatilization and redeposition of nitrogen) N_2O emissions from managed soils**.**

Italian N_2O emission from managed soils in the years 2010-2021 were simulated using the LPJ-GUESS and ORCHIDEE models and compared with the gridded N_2O emissions from WP2.1, used as priors in WP2.5, the so called “TNO-GHGco_v7_Avengers_countries” hereinafter referred to as WP2.2 priors (see Deliverable 2.2 for more details).

In addition to N input offered by the models, as input to modelling activity the same N input used in the inventory were used, in order to make the results of simulations comparable with inventory estimates and to make considerations about emission factors and their temporal and spatial variability.

2.5.1 Inventory estimate sector 3.D

The Tier 1 method of IPCC Guidelines for National GHG Inventories (IPCC 2019), hereinafter referred to as IPCC GL, assumes that N_2O emissions are directly proportional to the N amount added to the soil, with emission factors specific for N sources and types, and distinct for direct and indirect emission pathways:

- Direct N_2O emissions from managed soils that occur through a direct pathway
- Indirect N_2O emissions taking place through two indirect pathways: N volatilization/deposition and N leaching
- For both direct and indirect N_2O emissions the equations provided by the IPCC GL are used to estimate the amount of N lost with emissions (N_2O–N amount), which must be converted to N_2O emissions by using the following equation, where 44/28 is the ratio between molecular weights of N_2O and N: $N_2O = N_2O\text{–}N * 44/28$

A summary of the nitrogen inputs to soils taken into consideration for the estimate of direct and indirect N_2O emissions and their pathways are given in Fig. 2.

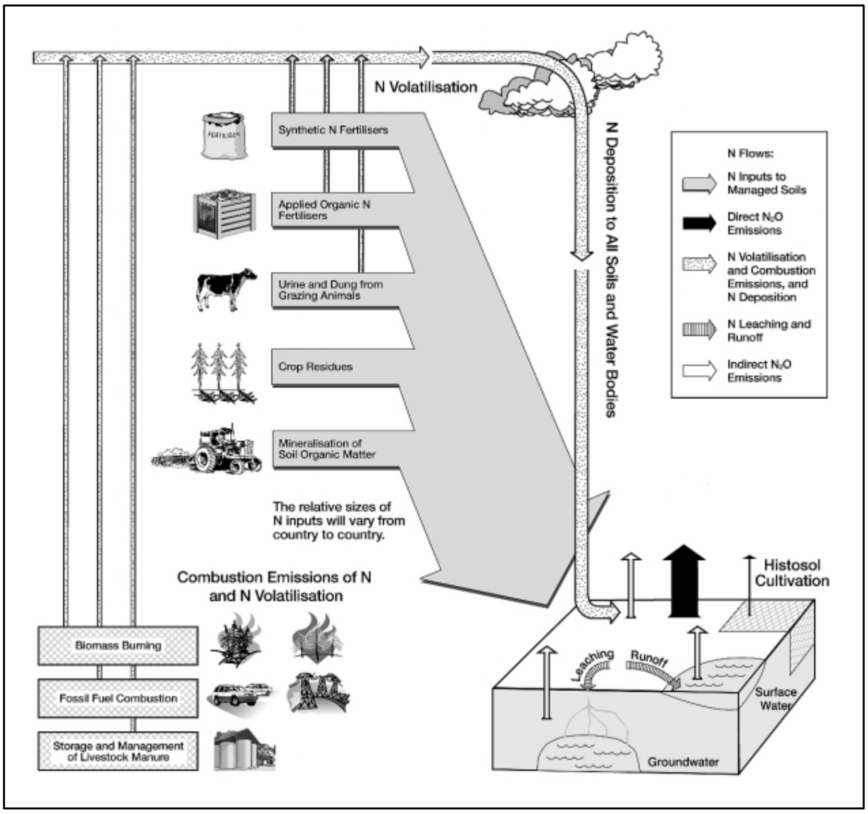

Figure 2. A summary of the nitrogen inputs to soils taken into consideration for the estimate of direct and indirect N_2O emissions and their pathways (from Figure 11.1 in Vol. 4 of IPCC GL).

The reference equation for calculation of direct N_2O emissions from managed soils in IPCC GL is Equation 11.1 (Chapter 11, Volume 4):

$$\mathbf{N_2O_{direct} - N = [(F_{SN}+F_{ON}+F_{CR}+F_{SOM}) * EF_1]+[(F_{PRP,CPP}*EF_{3PRP,CPP})+(F_{PRP,SO}*EF_{3PRP,SO})]}$$

where the following N inputs to managed soils are considered

- **F_{SN}** annual amount of synthetic fertilizers N applied to soils

- **F_{ON}** annual amount of organic fertilizers N applied to soils, composed of: **F_{AM}** animal manure, **F_{COMP}** compost, **F_{SEW}** sewage sludge, **F_{OOA}** other organic amendments as rendering waste, guano, brewery waste, etc.

- **F_{CR}** annual amount of N in crop residues (above-ground and below-ground), including N-fixing crops, and from forage/pasture renewal, returned to soils annually.

- **F_{SOM}** annual amount of N in mineral soils that is mineralized, in association with loss of soil C from soil organic matter as a result of changes to land use or management

- **F_{PRP}** amount of N in urine and dung deposited by grazing animals on soils on pasture, range and paddock (the subscripts CPP and SO refer to Cattle, Poultry and Pigs, and Sheep and Other animals, respectively)

Table 1. The emission factors for the estimation of direct N_2O emissions. Left column: from table 11.1 of Volume 4 of IPCC GL (IPCC, 2019). Right column: the Implied Emission Factors (IEF) used in Italian Inventory submission 2023 (Romano et al., 2023), derived from IPCC GL (IPCC, 2006)

	Tier 1 IPCC GL 2019 [kg N_2O–N (kg N)$^{-1}$]		**Uncertainty Range**	**IEF IT inventory (sub 2023) [kg N_2O–N (kg N)$^{-1}$]**	
EF_1	Aggregated value	0.010	0.001 – 0.018	Synthetic fertilizer inputs	0.0096
	Synthetic fertiliser inputs in **wet climates**[1] (including mixtures that include both synthetic and organic forms of N)	0.016	0.013 – 0.019		
	Other N inputs in **wet climates** (organic amendments, animal manures e.g. slurries, digested manures, N in crop residues and mineralised N from soil organic matter decomposition)	0.006	0.001 – 0.011	Organic fertilizer input	0.010
	All N inputs in **dry climates**[2]	0.005	0 – 0.011		
$EF_{3PRP, CPP}$	Aggregated value	0.004	0.000 – 0.014	Aggregated value	0.0111
	Wet climates	0.006	0.000 – 0.027		
	Dry climates	0.002	0.000 – 0.007		
$EF_{3PRP, SO}$	Aggregated value	0.003	0.000 – 0.010		

The reference equation for calculation of indirect N_2O emissions from atmospheric deposition of N volatilised from managed soils in IPCC GL is Equation 11.9 (Chapter 11, Volume 4):

$$N_2O_{(ATD)} - N = [(F_{SN} * Frac_{GASF}) + ((F_{ON} + F_{PRP}) * Frac_{GASM}] * EF_4$$

Where

- $Frac_{GASF}$ = fraction of synthetic fertiliser N that volatilises as NH_3 and NO_x

[1] Wet climates occur in temperate and boreal zones where the ratio of annual precipitation: potential evapotranspiration > 1, and tropical zones where annual precipitation > 1000 mm.

[2] Dry climate occur in temperate and boreal zones where the ratio of annual precipitation: potential evapotranspiration < 1, and tropical zones where annual precipitation < 1000 mm

- $Frac_{GASM}$ = fraction of applied organic N fertiliser materials (F_{ON}) and of urine and dung N deposited by grazing animals (F_{PRP}) that volatilises as NH_3 and NO_x

The reference equation for calculation of indirect N_2O emissions from N leaching/runoff from managed soils in IPCC GL is Equation 11.10 (Chapter 11, Volume 4):

$$N_2O_{(L)} - N = (F_{SN}+F_{ON}+ F_{PRP}+F_{CR}+F_{SOM}) * Frac_{LEACH-(H)} * EF_5$$

Where

- $Frac_{GASF}$ = fraction of all N added to/mineralised in managed soils in regions where leaching/runoff occurs that is lost through leaching and runoff

Table 2. The emission factors (EF) and fractions (Frac) for the estimation of indirect N_2O emissions, from table 11.3 of volume 4 of 1 IPCC GL for National GHG Inventories (IPCC, 2019) and the Implied Emission Factors (IEF) used in Italian Inventory submission 2023 (Romano et al., 2023).

<table>
<tr><th colspan="5">IPCC GL Refinement 2019</th><th colspan="2">IT inventory (sub 2023)</th></tr>
<tr><th>Default value</th><th>Uncertainty range</th><th>Disaggreg.</th><th>Default value</th><th>Uncertainty range</th><th colspan="2">IEF Value</th></tr>
<tr><td colspan="7">EF_4
N volatilization and redeposition [kg N_2O–N (kg NH_3–N + NO_x–N volatilized)$^{-1}$]</td></tr>
<tr><td rowspan="2">0.010</td><td rowspan="2">0.002 – 0.018</td><td>Wet climate</td><td>0.014</td><td>0.011-0.017</td><td rowspan="2" colspan="2">0.010</td></tr>
<tr><td>Dry climate</td><td>0.005</td><td>0.000-0.011</td></tr>
<tr><td colspan="7">$Frac_{GASF}$
Volatilization from synthetic fertiliser [kg NH_3–N + NOx–N) (kg N applied) $^{-1}$]</td></tr>
<tr><td rowspan="4">0.11</td><td rowspan="4">0.02 – 0.33</td><td>Urea</td><td>0.15</td><td>0.03-0.43</td><td rowspan="4" colspan="2">0.10</td></tr>
<tr><td>Ammonium-based</td><td>0.08</td><td>0.02-0.3</td></tr>
<tr><td>Ammonium-nitrate-based</td><td>0.05</td><td>0.00-0.20</td></tr>
<tr><td>Nitrate-based</td><td>0.01</td><td>0.00-0.02</td></tr>
<tr><td colspan="7">$Frac_{GASM}$
Volatilization from all organic N fertilisers applied, [kg NH3–N + NOx–N) (kg N applied) $^{-1}$]</td></tr>
<tr><td rowspan="3">0.21</td><td rowspan="3">0.00-0.31</td><td rowspan="3">-</td><td rowspan="3">-</td><td rowspan="3">-</td><td>Livestock excretion</td><td>0.09</td></tr>
<tr><td>Sewage sludge</td><td>0.12</td></tr>
<tr><td>Other organic fertilizers</td><td>0.08</td></tr>
<tr><td colspan="7">EF_5
[leaching/runoff] , kg N_2O–N (kg N leaching/runoff)$^{-1}$</td></tr>
<tr><td>0.011</td><td>0.000 – 0.020</td><td>-</td><td>-</td><td>-</td><td colspan="2">0.0075</td></tr>
<tr><td colspan="7">$Frac_{LEACH-(H)}$
N losses by leaching/runoff in wet climates, [kg N (kg N additions or deposition by grazing animals)$^{-1}$]</td></tr>
<tr><td>0.24</td><td>0.01 – 0.73</td><td>-</td><td>-</td><td>-</td><td colspan="2">0.27</td></tr>
</table>

2.5.2 Spatialized N input elaborated from inventory activity data

As input to modelling, the historical time series 2010-2021 of Nitrogen input to soil, elaborated for the Italian inventory, was used to make the simulation more comparable with inventory data. The aim of the simulations was to detect spatial and temporal variability in emissions and emission factors.

Provincial disaggregation and gridded emissions were available only for 2010, 2015 and 2019 (reference years). Where no spatially distributed emissions were available, the spatial distribution of the closest available reference year was used. Specifically, for 2011 and 2012 the spatial distribution from 2010 was used, for 2013 and 2014 the spatial distribution from 2015 was used, and for 2016-2021 the spatial distribution of 2019 was used. For missing years, the N input per province was calculated as the product of the national N input (CRF submission 2023) and the percentage contribution of that province in the reference years.

The methodologies and proxies used to disaggregate N input at NUTS3 level (Italian provinces) are described in the ISPRA report (Taurino et al., 2022).

Moreover, the NUTS3 level N inputs were disaggregated on the EMEP grid (0.1°x 0.1°), considering the land use of each grid cell (Fig. 3&4). To do so Corine Land Cover (CLC) 2012 (for years 2010-2015) and CLC 2018 (for years 2016-2021) were used. Using ARCGIS Pro, F_{SN} (synthetic fertilizers) were distributed only on cropland (CLC class codes 211, 212, 213, 221, 222, 223, 241, 242), F_{PRP} on grassland (CLC class codes 231, 321, 333, 243 e 244), while organic N inputs (F_{AM}, F_{COMP}, F_{SEW}, F_{CR}) on both cropland and grassland.

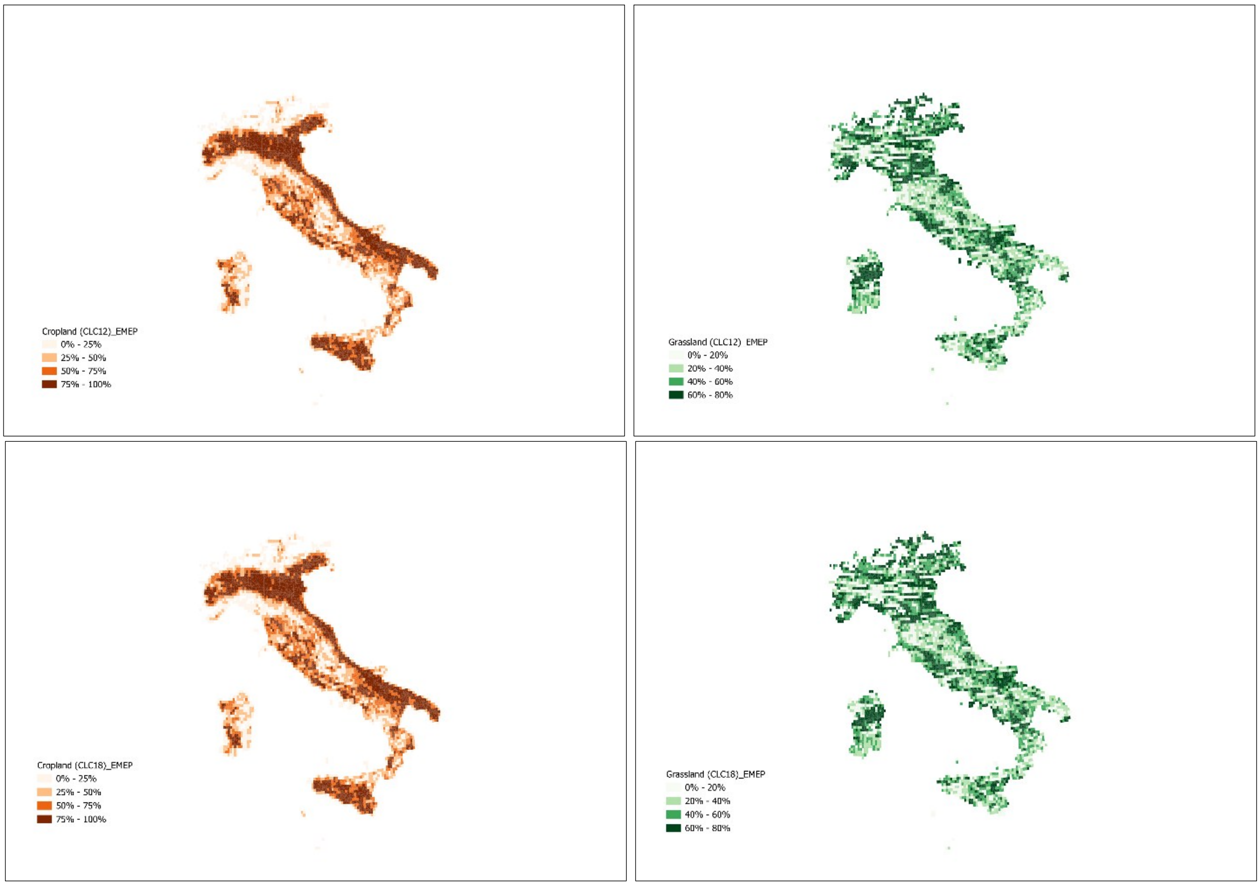

Figure 3. The percentage coverage of cropland and grassland classes in the EMEP 0.1° grid cells as classified with the CLC 2012 and CLC 2018 products

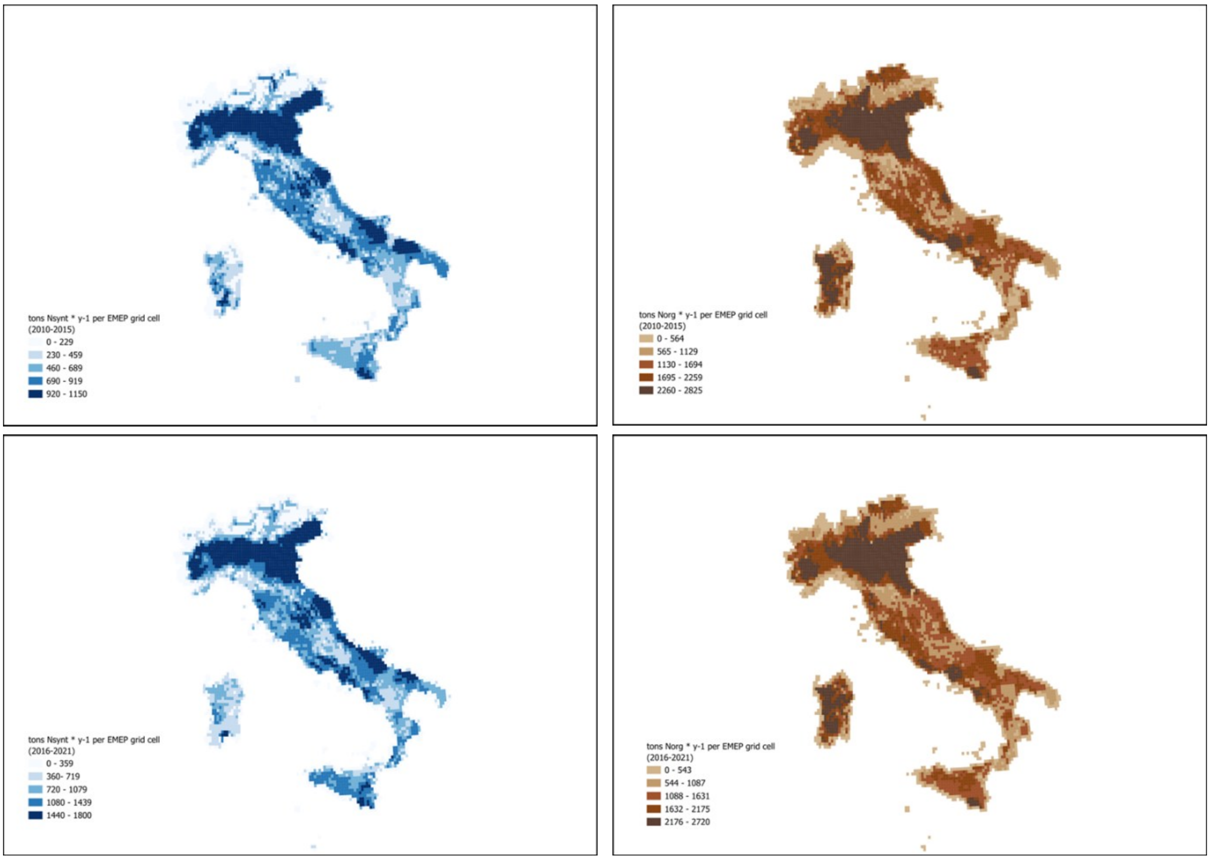

Figure 4. Estimated amount (tons) of synthetic and organic fertilizers per 0.1° EMEP grid cell, represented as average for 2010-2015 and 2016-2021.

2.5.3 LPJ-GUESS model setup

For the Italian case the main branch of LPJ-GUESS was used (LPJ-GUESS v4.1, trunc branch, revision 13203). A detailed description of the N transformations and evaluation of N_2O fluxes is provided by Ma et al. (2025). The mineral fertilizer is assumed to have equal amounts of NH_4^+ and NO_3^- and is added to the soil water. The manure is added to the soil organic matter pool together with associated carbon, assuming a 30:1 C/N ratio (Olin et al., 2015). The fertiliser is added at two occasions per year with the total annual amount divided equally between the two dozes. For cropland, the dates are set when the development stage (0-2) according to Wang and Engel (1998) has passed 0.5 (after terminal spikelet is out) and 0.9 (start of heading stage) respectively. For the grassland simulations, the dozes were given at fixed dates, set to the first of April and the first of June.

In the cropland simulation for Italy, the following CMIP6 (Hurtt et al., 2020) crop types were assessed:

- "CC3ann" C3 annual, in LPJ-GUESS mapped as winter wheat (no inter-crop grass)
- "CC3per" C3 perennial, in LPJ-GUESS mapped to summer wheat with inter-crop grasses enabled
- "CC3nfx" C3 nitrogen fixer, in LPJ-GUESS mapped to summer wheat (no inter crop grass)
- "CC4ann" C4 annual, in LPJ-GUESS mapped to corn (no inter crop grass)

For each of these types there was also an irrigated variant.

From the ISPRA land-use and fertilisation data, the amounts per square meter was calculated for each simulated 0.5-degree grid cell. For the spinning up the model CMIP6 fertilisation data (Hurtt et al., 2020) were used. A quality check of the match between CMIP6 data and the ISPRA data for the overlapping period (2010-2021) was done. If the mean ISPRA amount divided by the mean CMIP6 amount for 2010-2021 was between 1/3 and 3, this quotient was used to scale the CMIP6 data for 1850-2009 and 2022 and the inventoried data were used for 2010-2021 (this criterion was passed for 146 of 161 gridcells, representing 92% of the area). If the quotient was out of the range (1/3 - 3), the CMIP6 data were used directly for 1850-2009 and 2022, and for the period 2010-2021 the annual deviation from the 2010-2021 mean of the inventoried data was used to scale the CMIP6 data. To distribute the fertiliser between the crop types the relative CMIP6 amounts were used.

The grassland area was simulated as pastures. In these C3 and C4 grass are competing but in the Italian climate C3 grass was always the stronger and there was no simulated C4 biomass. Harvest from pastures is in the form of grazing animals which annually eat 50% of the aboveground biomass. However, to mimic that a large fraction of N in the grazed biomass soon returns to the system as urine, only 25% of N in the harvested biomass leaves the system and the remaining 75% is added to the leaf litter N pool (Ma et al., 2025).

For scaling up to country totals, the ISPRA land-use data for 2012 were used for the period 2010-2015 and the 2018 data were used for 2016-2022. To evaluate the added value of using the country specific ISPRA, the results were also compared with the Avengers D2.2 report data (chapter 4 – Natural Fluxes), in which the CMIP6 data were used for both land-use and fertilisation.

2.5.4 ORCHIDEE model setup

For ORCHIDEE, the model spin-up and historical simulation was run at 0.5 x 0.5 degrees resolution. These simulations use a land cover map delineating 15 PFTs (2 crop PFTs, 8 tree PFTs, 4 grassland PFTs, and the bare soil PFT). The ORCHIDEE PFT map is based on the ESA CCI Land Cover map v2.0.7b for 2010 aggregated using a cross-walking table to 15PFTs at 0.25degrees. The meteorological forcing data used the CRUJRA v2.4 data product.

The spin-up recycled 1971-1990 meteorological forcing for 340 years to allow the soil nitrogen and carbon pools to reach equilibrium. For the historical simulation fertilizer using the NMIP2 product (Tian et al. 2022), atmospheric N deposition (NHx-N and NOy-N) was from the International Global Atmospheric Chemistry (IGAC)/Stratospheric Processes and Their Role in Climate (SPARC) Chemistry–Climate Model Initiative (CCMI) N deposition fields (Tian et al. 2018), and BNF inputs were used. During the spin-up simulation, nitrogen inputs for the year 1850 were recycled using the same nitrogen input products. Before beginning the historical simulation, a transient simulation is used to prepare for current meteorological conditions (1801 - 2010) recycling the 1991 – 2010 meteorological forcing. The representation of the nitrogen cycle in ORCHIDEE has been extensively described and evaluated (Vuichard et al. 2019).

For the period, 2010-2022, two historical simulations were created using 1) NMIP2 nitrogen inputs, and 2) a simulation using the ISPRA nitrogen inputs and corresponding CORINE land use map.

2.5.5 LPJ-GUESS output data

Raw ASCII-format output files, ncdf-files of key variables compiled to 0.5° grid, and files for the setup of the simulations are stored at ICOS Carbon Portal fileshare (https://fileshare.icos-cp.eu/apps/files/files/4880159?dir=/AVENGERS/WP4-Process_modelling/Tasks/Task%204.1%20documentation/Model%20output%20data/LPJGUESS/ItalyCaseStudy). Further details are given in the ReadMe file of the directory.

2.5.6 ORCHIDEE output data

The model results are stored as ncdf-files divided in vegetation and soil carbon output (SBG, stomate*.nc) and energy and water budget output (SRF, sechiba*.nc) at ICOS Carbon Portal fileshare (https://fileshare.icos-cp.eu/apps/files/files/4867313?dir=/AVENGERS/WP4-Process_modelling/Tasks/Task%204.1%20documentation/Model%20output%20data/ORCHIDEE). Further details are given in the ReadMe file of the directory.

3 Forest case study Sweden – results and discussion

3.1 Country part and county specific estimates on carbon stock-changes

The simulated levels of the different components of carbon emissions, based on a stock-change accounting, from forests in Sweden compare reasonably well with the inventory-based reported numbers (Fig. 5). In particular, the vegetation and litter components show much larger variation in the simulations than in the reported values, which are based on 5-year inventory cycles of permanent plots. Both models indicate a relatively small uptake or a release from soil, ranging from -10 to +10 Mton CO_2 per year, whereas the inventory shows a steady uptake of approximately 15 Mton per year. The varying sizes of 10-year classes in the initialisation of LPJ-GUESS (see Annex 1) lead to differences in the simulation outputs across different periods, most clearly seen in the flux from harvested products.

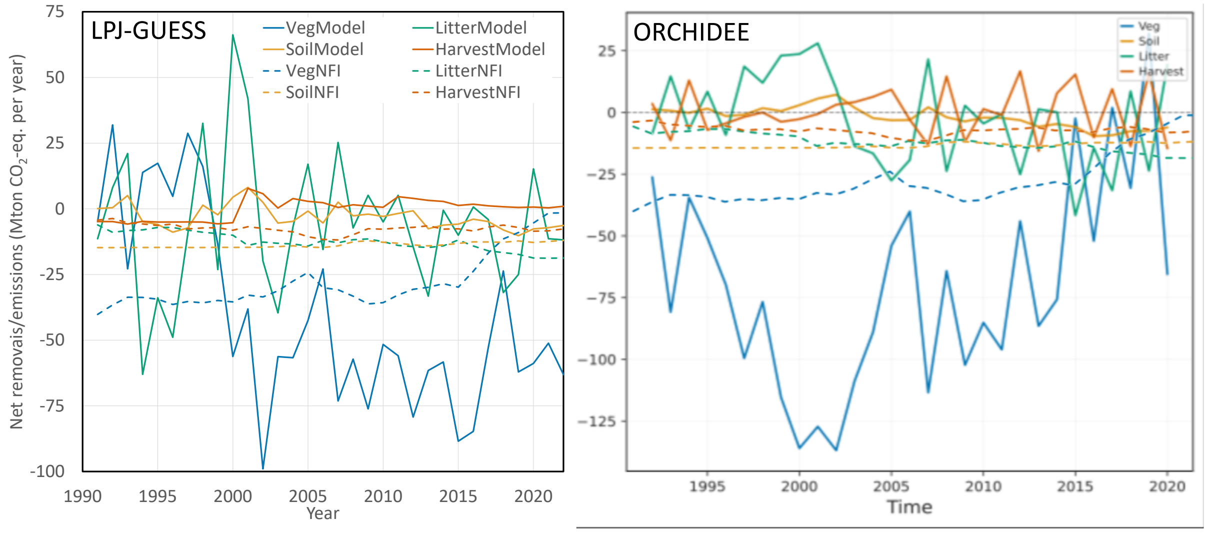

Figure 5. Total annual emissions from forest in Sweden divided into different components as modelled by LPJ-GUESS and ORCHIDEE compared to data from the national report based on inventory data. Only carbon related fluxes are represented. All emissions are based on a stock-change accounting (carbon previous year – carbon stock current year). The harvest stock changes depend on harvested biomass and longevity of different wood products.

When examining the simulated net change in vegetation carbon for different parts of Sweden and various forest or plant functional types (PFTs), the interannual variation becomes even more apparent (Fig. 6). The influence of weather and management is explored further in the following sections.

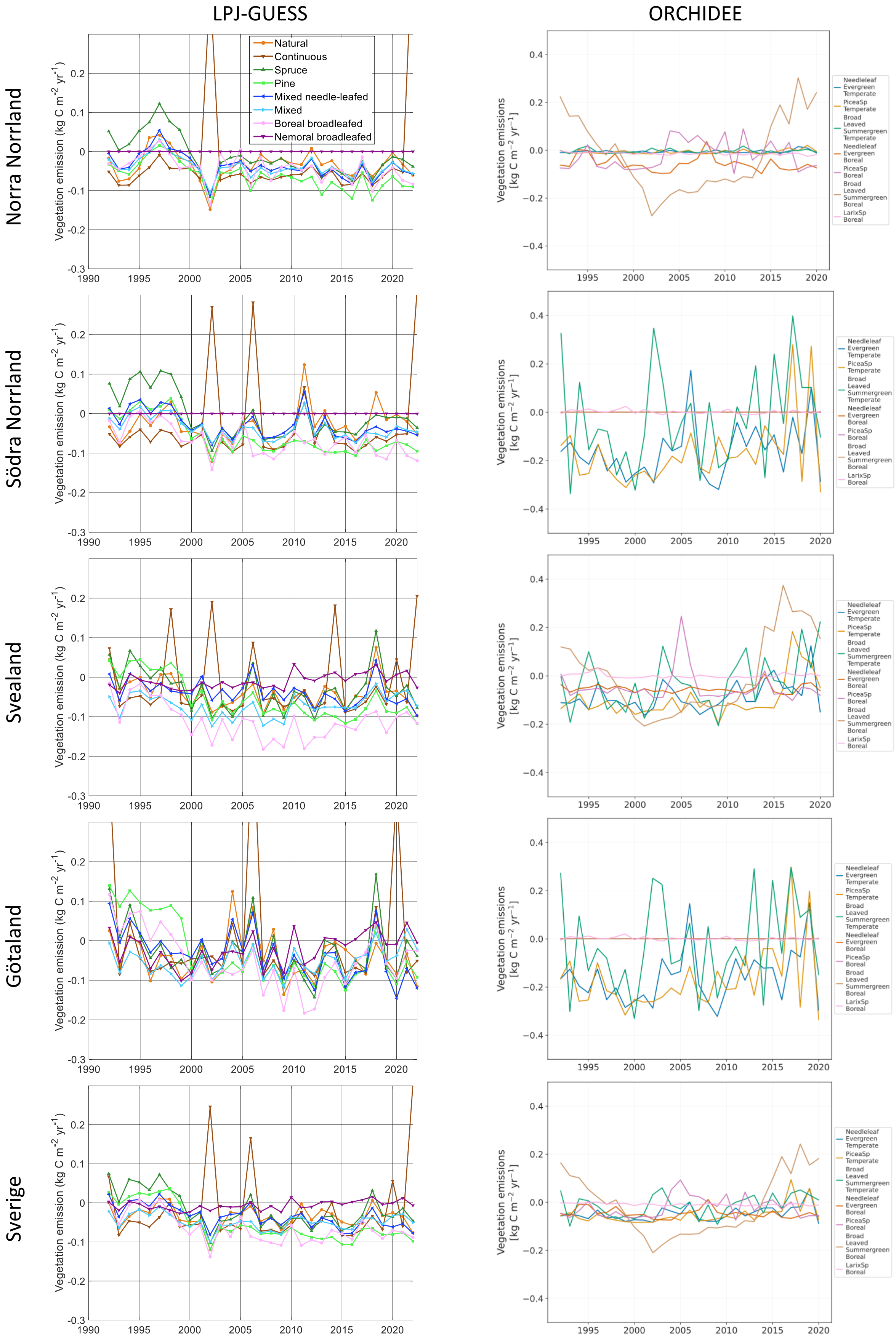

Figure 6. Net emissions from the vegetation of different forest types, calculated from the change in simulated standing biomass across country parts (Fig. 1). In the LPJ-GUESS simulations all continuous

cover forest of a certain cutting interval (Figure 1) is cut in the same year, which explains the peaks in those simulations.

3.2 Impacts of weather and climate extremes

The dry years of 2006 and 2018 (Fig. 7) show a large reduction in the vegetation sink in Svealand and a shift to net emissions in Götaland (Fig. 6). The simulations showed that spruce-dominated forests were more affected than broad-leafed types. The 2018 SPEI drought index (Fig. 7) aligns with the reduction in the NEE sink (Fig. 8). Modelled estimates of the sink reduction are up to 0.3 kg C m^{-2} for LPJ-GUESS and up to 0.4 kg C m^{-2} for ORCHIDEE. These results agree with eddy covariance observations, where two spruce forests in Götaland had reductions of 0.39 and 0.25 kg C m^{-2}, respectively (Lindroth et al. 2020). In Norra Norrland, the drought was more severe in 2006 than in 2018 (Fig. 7), which is reflected in a sink reduction in 2006 and a normal or above-average sink in 2018 (Fig 6 & 8). Lindroth et al. (2020) concluded that a moderately warm and dry summer could have a positive effect on productivity in the temperature limited ecosystems of northern Scandinavia.

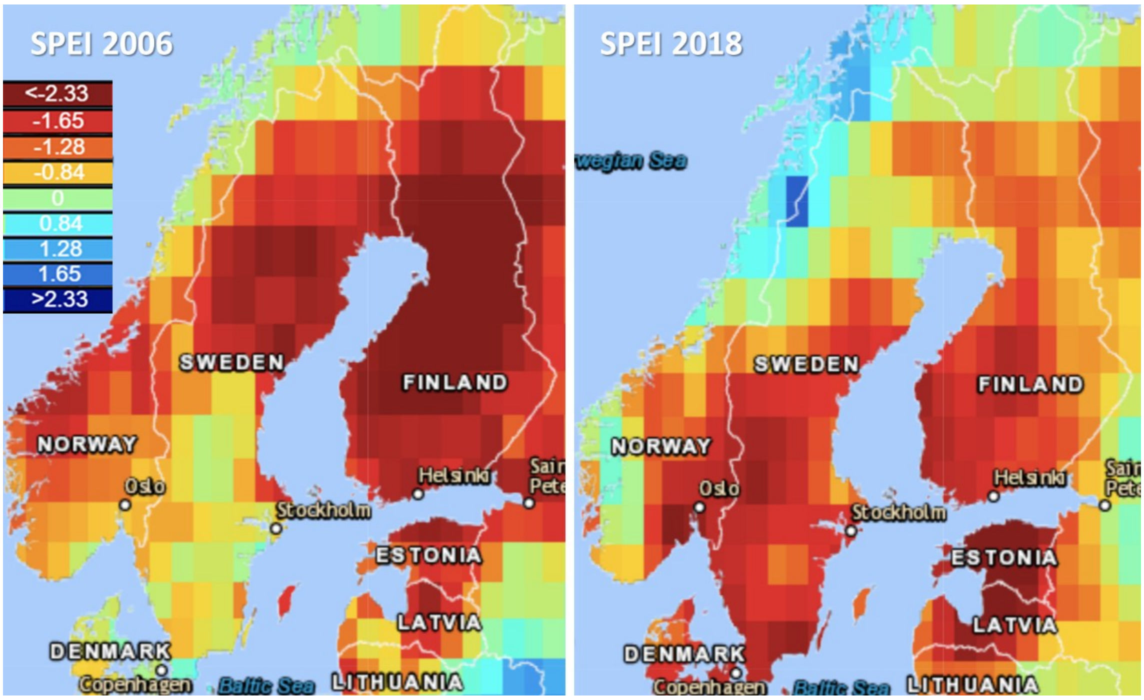

Figure 7. Map of SPEI June-August drought index from Global Drought Monitor () during the summers of 2006 and 2018 (April–September).

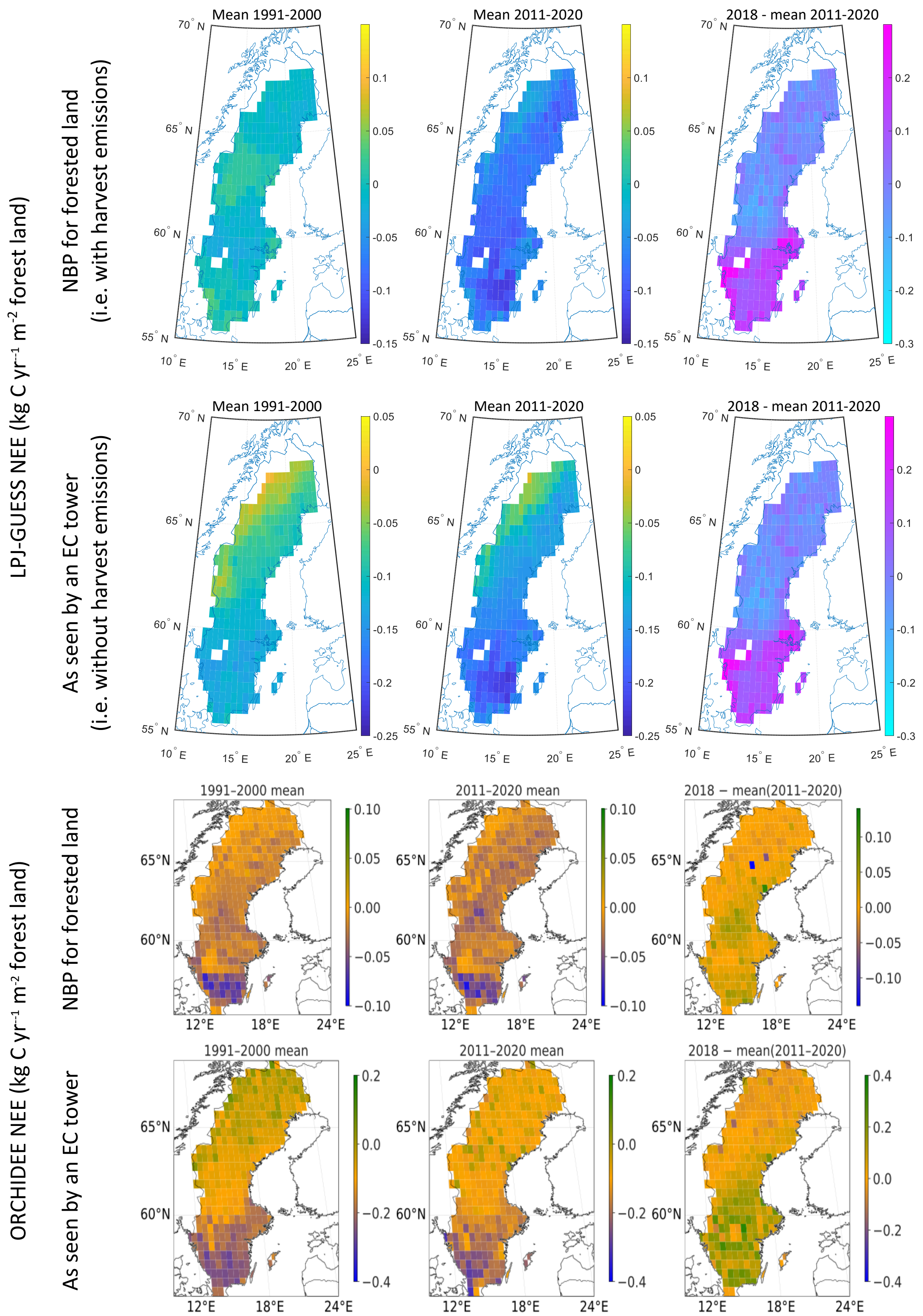

Figure 8. Maps of average simulated NEE over two 10-year periods, and the difference between the in south Sweden extremely dry year 2018 and the 10-year mean. Negative values indicate CO_2 uptake by the forest. Note that the LPJ-GUESS simulations include a storm and bark beetle disturbances while ORCHIDEE was run without disturbances. Results are presented both including and excluding harvest emissions.

Damage from storm and spruce bark beetles was explicitly modelled in LPJ-GUESS (Fig. 9). Norway spruce is the most wind-sensitive PFT, but spruce monocultures show average storm sensitivity only. The sensitivity is underestimated, especially in Götaland, because the simulated stands are denser and the trees shorter and thinner than observed (Fig. 12). In natural, continuous, and mixed forest, the spruce PFT has lower density, and the lower within-PFT competition leads to taller trees and high storm sensitivity. Spruce bark beetle damage depends on insect phenology and availability of brood trees (>15 cm in diameter). The outbreak dynamics following the storms in 2005 and 2007, and the 2018 drought, are relatively well captured for Götaland. The modelled damage, up to 0.2 kg C m^{-2}, did not have an obvious impact on the vegetation carbon sink (Fig. 6).

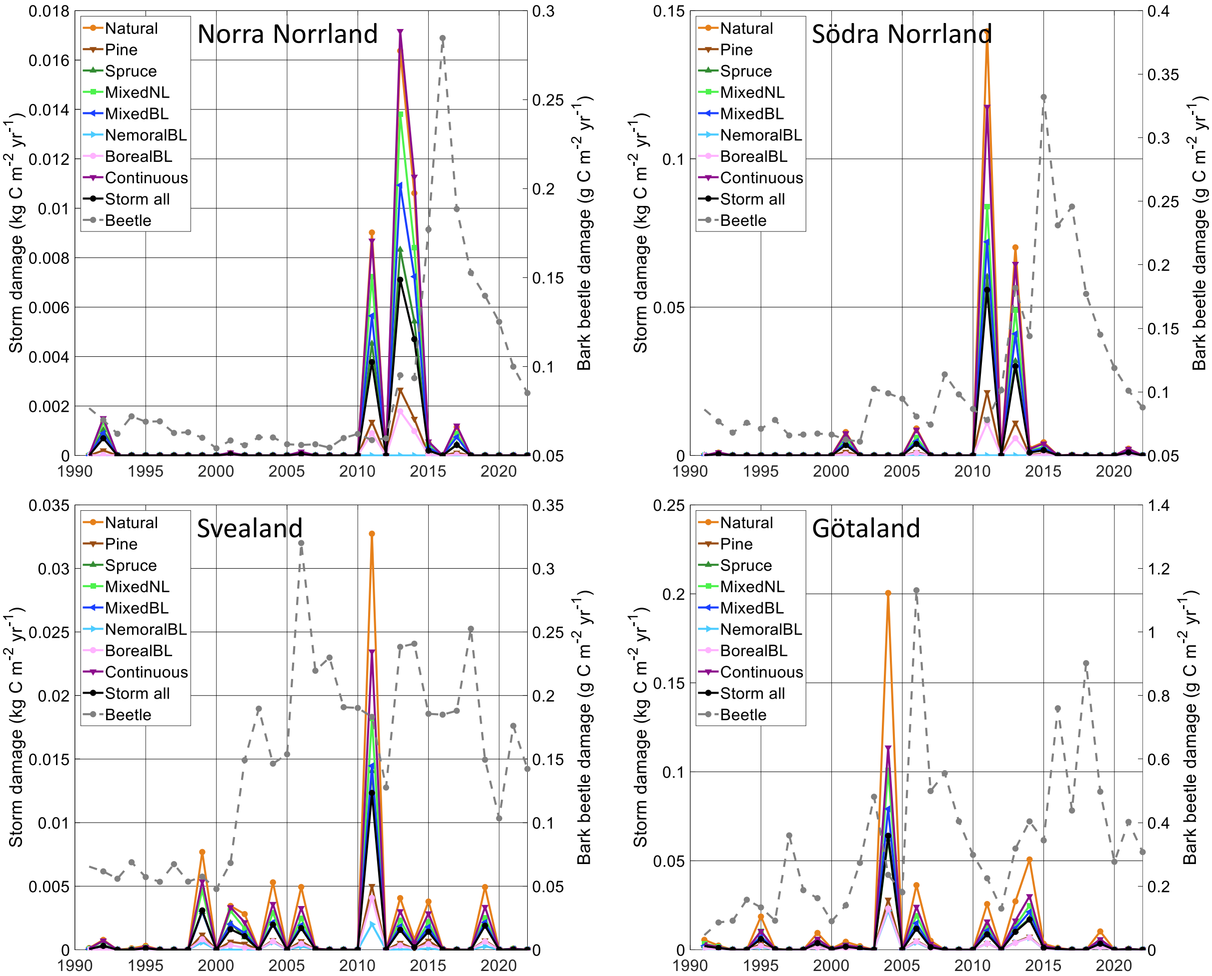

Figure 9. Biomass mortality due to storm and bark beetle damage (left and right axis, respectively; note the different unit) as simulated with LPJ-GUESS for different parts of Sweden. For the storm damage the level for different forest types is presented as well as the average for all (black line).

3.3 Estimated impact of different management methods

According to LPJ-GUESS simulations, broad-leafed forest types are strong carbon sinks, and pine forests are the most efficient carbon sequesters in the northern counties. In contrast, spruce-dominated forest types (spruce, mixed needle-leafed, continuous, and natural) are weaker sinks (Fig. 10, Annex Fig A2). The simulated rotation period is shortest for the boreal broad-leaf forests followed by spruce, and longest for nemoral broad-leaf forest. However, this has no clear impact on the vegetation carbon sink. According to the ORCHIDEE simulations, the broad-leafed summergreen PFT is the strongest sink in the boreal counties, while the Spruce PFT is strongest in Svealand and Götaland counties (Fig. 10). The large differences in modelled vegetation sink strength between forest types and PFTs reflect model uncertainty.

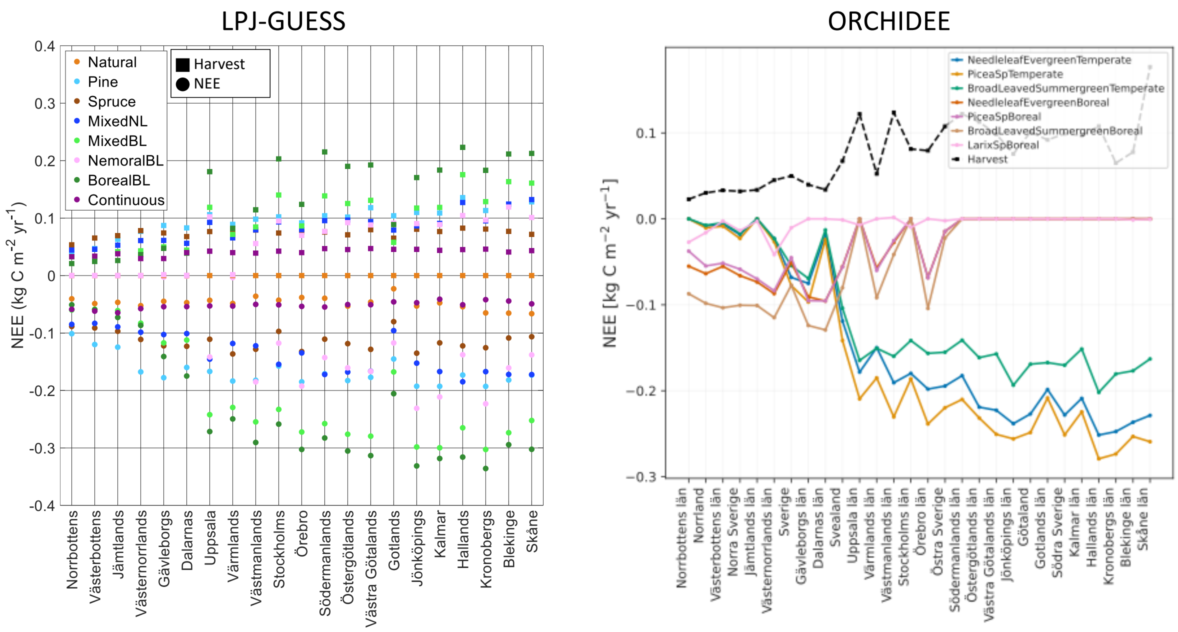

Figure 10a. NEE excluding harvest, and carbon removed by harvest, averaged over 1990-2020 for different forest types (LPJ-GUESS) and plant functional types (ORCHIDEE). The LPJ-GUESS harvest numbers represent carbon removed from the forest. In ORCHIDEE, harvested wood enters short, medium, or long-lived product pools, and emissions are subsequently calculated for these pools rather than for each PFT separately. Time series of these results are presented in Annex Fig A2.

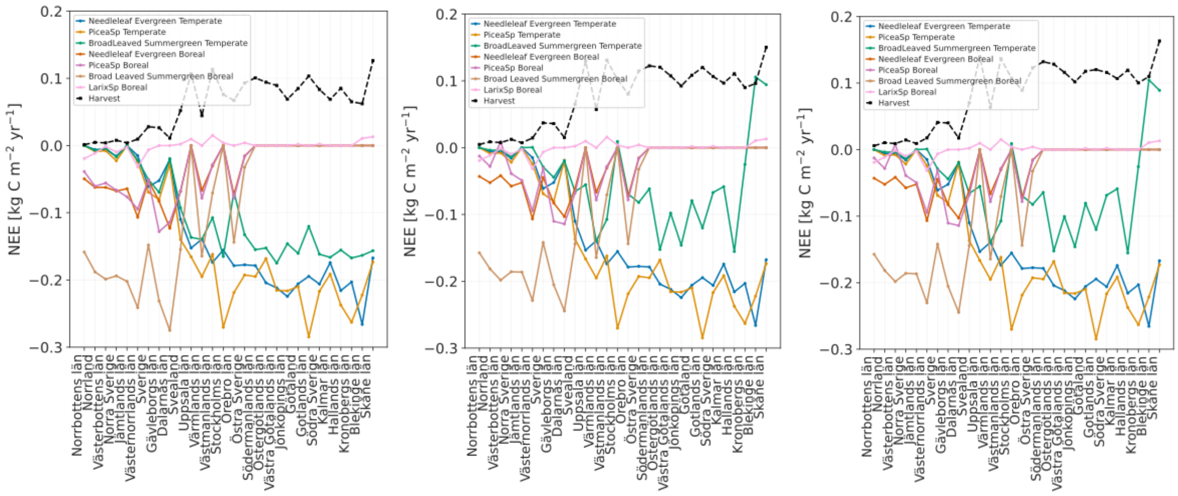

Figure 10b. NEE excluding harvest, and carbon removed by harvest, averaged over 2020-2100 under ssp370 for different plant functional types (ORCHIDEE) from simulations with unmanaged forests (left), high stand management (middle), and continuous cover forestry (right). In ORCHIDEE, harvested wood enters short, medium, or long-lived product pools, and emissions are subsequently calculated for these pools rather than for each PFT separately.

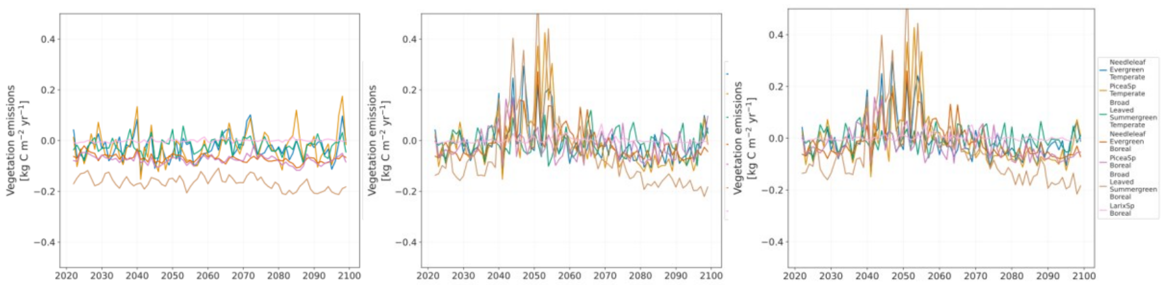

Figure 10c. Net emissions from the vegetation of different PFTs under different forest managed scenarios - unmanaged (left), high stand management (middle), and continuous cover forestry (right) - under future climate scenario ssp370, simulated by ORCHIDEE, calculated from the change in simulated standing biomass across country parts.

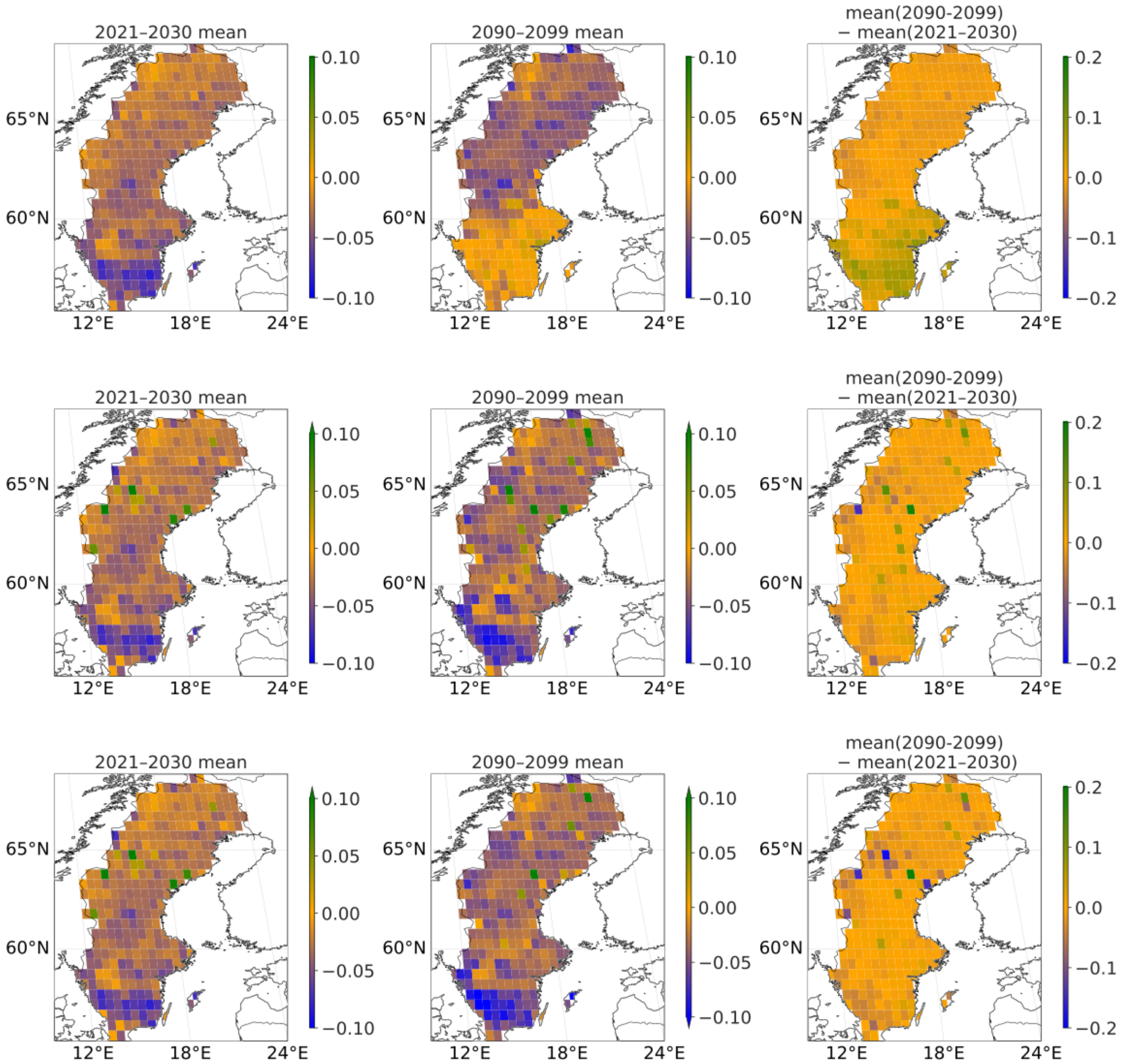

Figure 10d. Maps comparing average simulated NEE (including harvest) over two future 10-year periods under climate scenario ssp370 simulated with ORCHIDEE. Unmanaged forests (upper), high stand management (middle), and continuous cover forestry (lower).

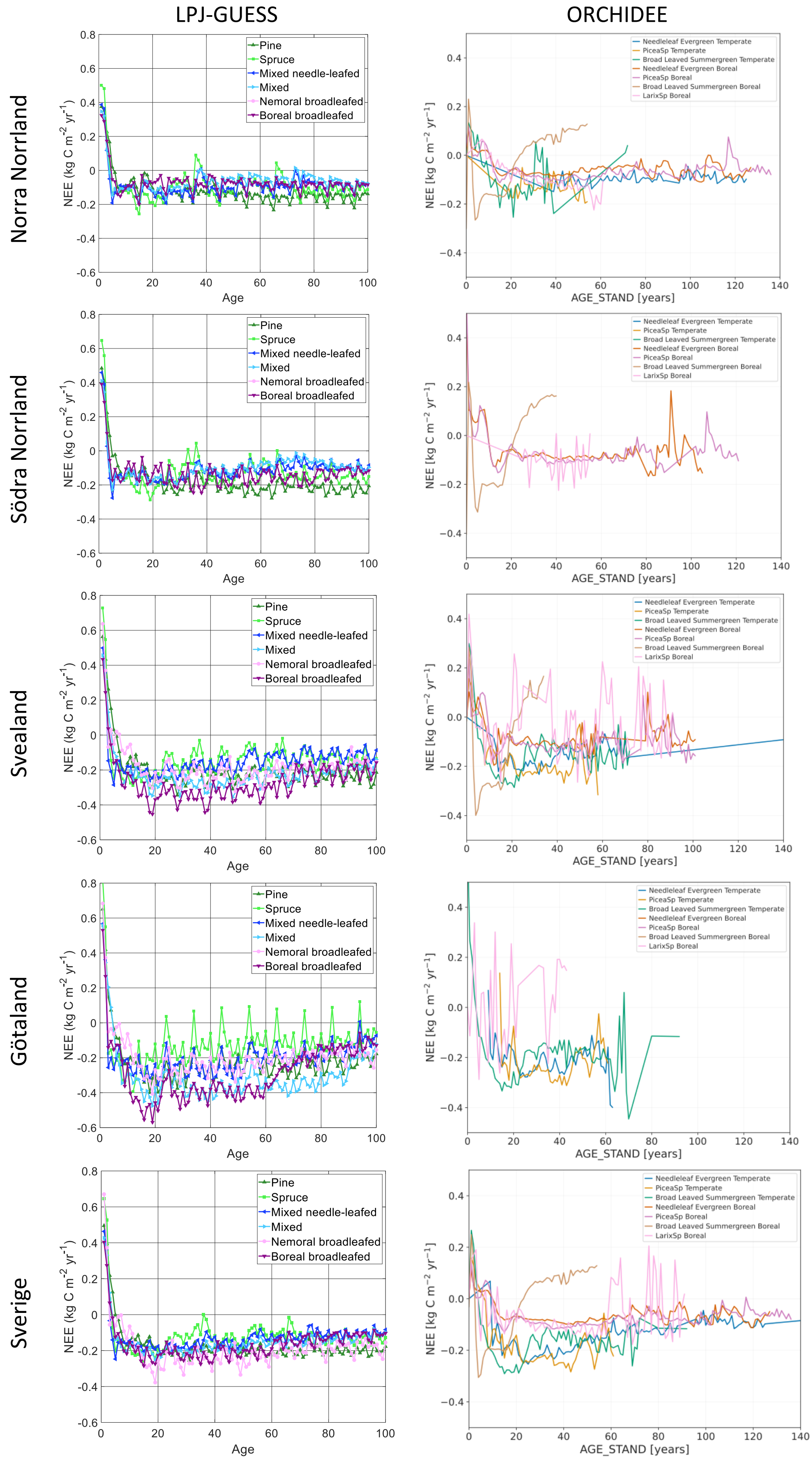

Figure 11. NEE emissions (excluding harvest) by age for the different even-aged forest types (LPJ-GUESS) or plant functional types (ORCHIDEE) across Sweden (Figure 1). For LPJ-GUESS, simulations

were run for age classes in 10-year intervals (complementary run, see Annex 1) and the results represent NEE for the years 2013-2022. The ORCHIDEE simulations were run using a single age-class, therefore, data for the entire model simulation (1991-2021) were used to illustrate the relationship.

Age is a key factor influencing carbon balance (Lindroth et al. 2009, Grelle et al. 2023), as shown in LPJ-GUESS simulations of even-aged forestry with clearcutting (Fig. 11). In the first year after clear-cutting, forest acts as a carbon source, emitting 0.35-0.7 kg C m^{-2}. It takes 3-6 years to turn into a sink, which is substantially shorter than the 8–13 years reported in eddy-covariance studies (Grelle et al. 2023). In Svealand and Götaland, carbon uptake peaks at 15–30 years of age and then gradually declines. Though uptake is lower in Södra and Norra Norrland, no clear trend is observed in the 5-100-year age span. One reason for the rapid modelled recovery is that the simulations include consistent, successful regeneration with rather large saplings. According to these model results, longer rotation periods would increase carbon sequestration. ORCHIDEE simulations also show that forests act as a carbon source after establishment, where the time taken for the forest to switch to a carbon sink depends on species/PFT with broadleaf boreal PFTs becoming a sink as soon as three years whereas needleleaf boreal PFTs become a sink after 10 years. Carbon uptake is generally greatest between 3 and 60 years of age.

In LPJGUESS, the differences between continuous cover forestry and natural forestry are small. However, continuous cover forestry leads to a larger carbon sink in the north of the country whereas natural forestry leads to a larger sink in the south of the country (Fig 10a). In ORCHIDEE, high stand management and continuous cover forestry lead to relatively similar carbon emissions relative to the emissions associated with unmanaged forests, when averaged over the remainder of the century (Fig 10b). Under the unmanaged forestry scenario, carbon lost from changing vegetation biomass tends to remain relatively consistent throughout the rest of the century. Whilst this is also true under both high stand management and continuous cover forestry for the beginning and end of the century, forestry becomes a carbon source in the 2040-2055 period under both these forest management scenarios (Fig 10c). Comparing the near-future and the end of century NEE emissions, shows that high stand management and continuous cover forestry leads to similar effects, where forestry across most parts of Sweden is a carbon sink and the south of Sweden is larger sink compared to the north (Fig 10d). Unmanaged forests, however, lead to the norther of Sweden becoming a larger sink compared to the south.

3.4 Tree standing volume and growth: uncertainty assessments

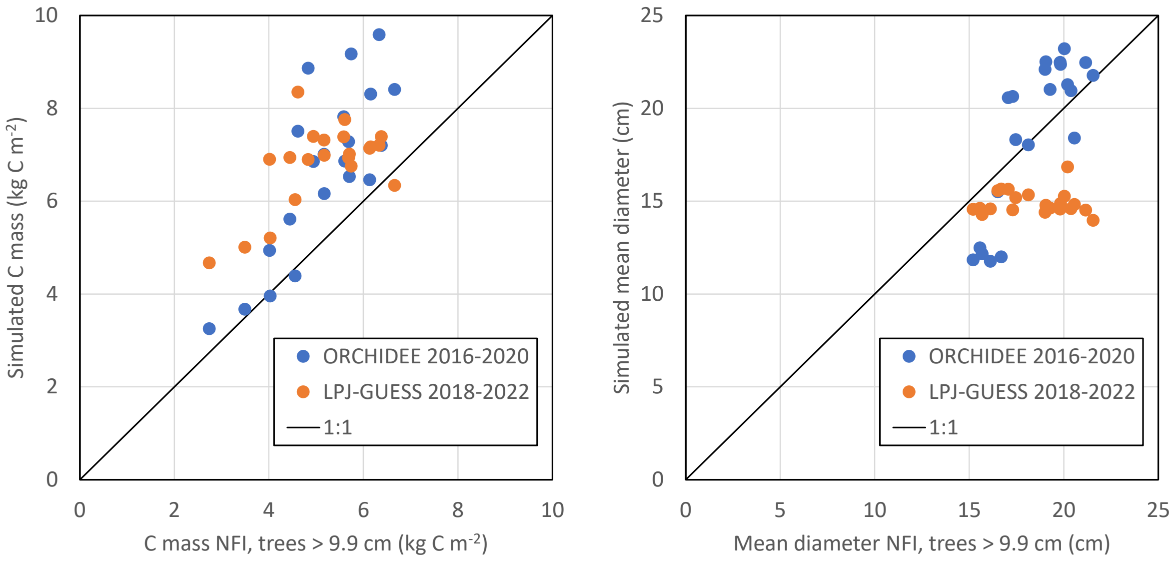

Figure 12. Simulated mean biomass by county compared to NFI data. Note that the NFI data includes only trees with a diameter greater than 99 mm, whereas the LPJ-GUESS include all tree biomass and ORCHIDEE include all biomass including understory vegetation.

Modelled forest carbon mass shows reasonable agreement with inventory-based estimates (Figure 12 & 13), with differences partly attributable to the varying definitions of biomass. The resulting biomass is influenced by tree growth and mortality driven by competition, age, disturbances, and forest management, all of which involves uncertainties and model simplifications.

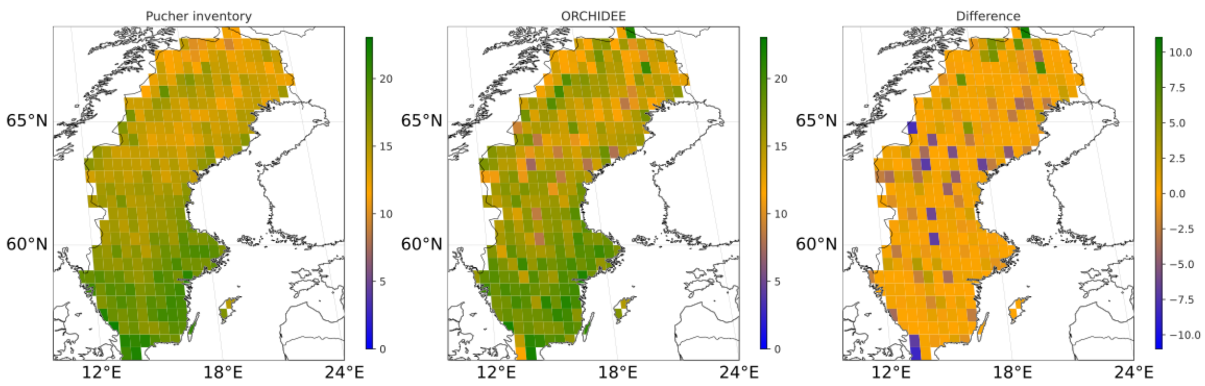

Figure 13. Comparison between ORCHIDEE simulation results and the Pucher inventory data (Pucher et al 2022) for tree diameters in the year 2005.

3.5 Soil carbon: uncertainty assessments

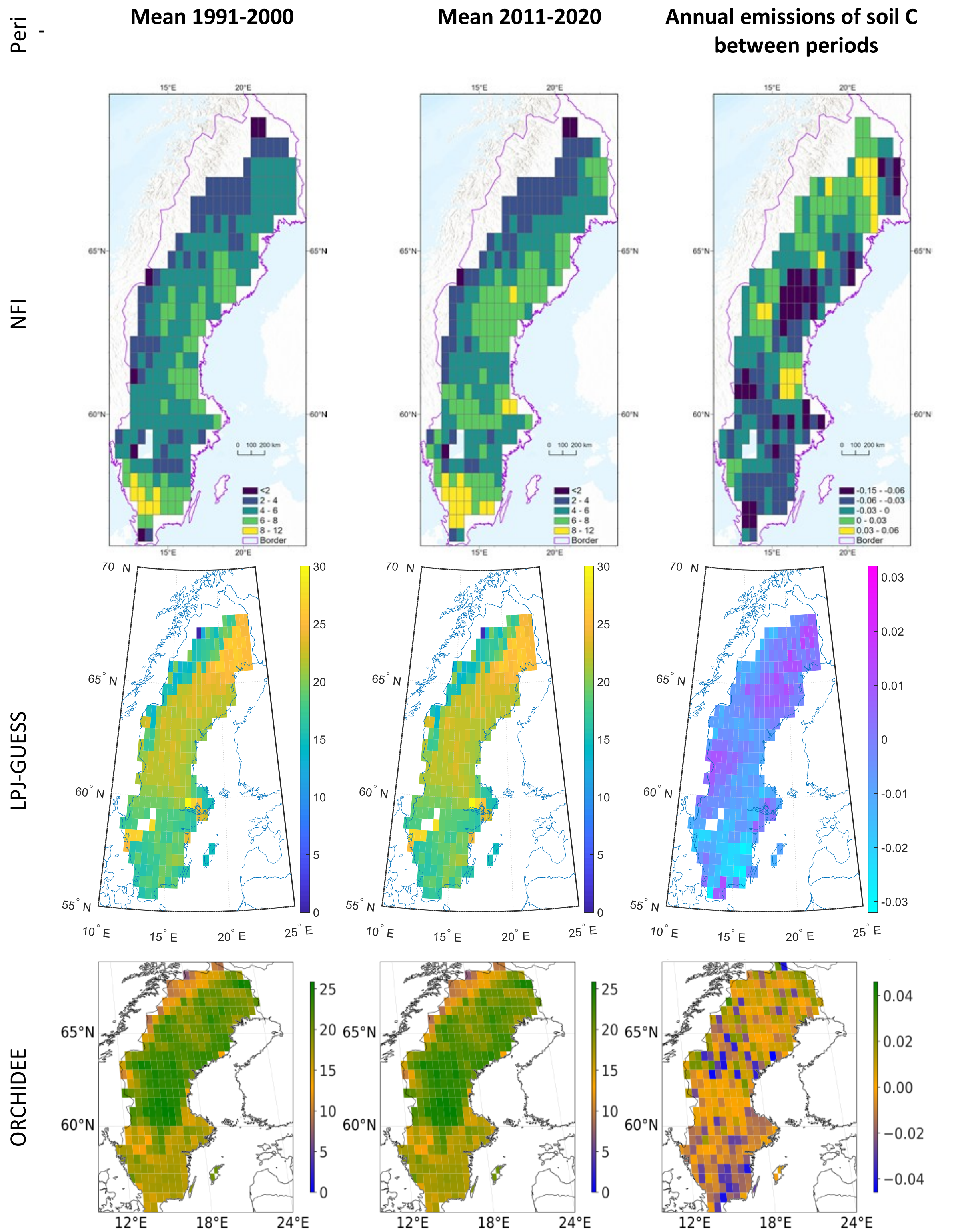

Figure 14. Observed and simulated soil and litter carbon pools on forest land for two 10-year periods (kg C m^{-2}, per unit forest land), and the mean annual release of soil carbon calculated from the difference between the periods (kg C m^{-2} yr^{-1}). It should be noted that reliable observed soil carbon stock data from the Swedish National Forest Inventory are available from 2003 onward since a significantly abrupt change in soil carbon stocks shows after 2003 (discussion with Prof. Erik Karltun).

To clearly depict both the spatial distribution of soil carbon stocks and their changes over time, results from the two 10-year period inventories during 2003–2022 are presented here for comparison with model simulations.

Both models simulate soil and litter carbon stocks that are high compared to inventory-based values (Fig. 14). The simulated stocks are also higher in north than in south, except in the NW-areas in or close to the Scandinavian mountains. A comparison between the two 10-year periods of 1991-2000 and 2011-2020 shows similar absolute values between the two model simulations, with carbon uptake in parts of southern and central Sweden, and the strongest emissions occurring in the north. These emissions range of -0.04 to 0.04 kg C m^{-2} yr^{-1} and can be compared to inventory-based estimates for soil carbon (Fig. 5), which indicate an average uptake of 0.03 kg C m^{-2} yr^{-1}.

Inventories-based soil carbon stock data presented here were generated from plot-level soil carbon stocks data derived from Swedish National Forest Inventories and integrated into 0.5-degree gridded maps using a 10 m resolution national land cover map. As noted, simulated soil carbon stocks from models generally exceed those from inventories, primarily due to differences in the soil depth represented. Specifically, LPJ-GUESS and ORCHIDEE simulate soil depths of 1.5 m and 2 m, respectively, whereas the Swedish National Forest inventories investigate soil to a depth of 0.5 m. Despite this discrepancy in magnitude, both model simulations and inventory data indicate a temporal increase in national soil carbon stocks (see Fig. 5 and Fig. A5 in the Appendix). The mean increase rate derived from the inventory data is 0.02 kg C m^{-2} yr^{-1} (Fig. A5), consistent with that from model simulations (0.03 kg C m^{-2} yr^{-1}). In addition, similar to model simulations, inventories also exhibit a general increase in soil carbon stocks in southern and central Sweden, and the largest decrease in the north.

4 Agricultural case study Italy – results and discussion

Italian N_2O emission from managed soils in the years 2010-2021 were simulated using LPJ-GUESS and ORCHIDEE models and compared with gridded N_2O emissions described in deliverable 2.2 (“*TNO-GHGco_v7_Avengers_countries”* hereinafter referred to as WP2.2 priors).

4.1 Fertiliser input

The fertilisation input to cropland and grassland soils uses the data provided by ISPRA at 0.1° grid cells level (Fig. 4 and Fig. 15b); these data were re-gridded on a 0.5° grid for both models (Figure 16). For both models the total manure added is assumed to be evenly distributed over the total cropland and grassland area and the grassland receives no mineral fertiliser.

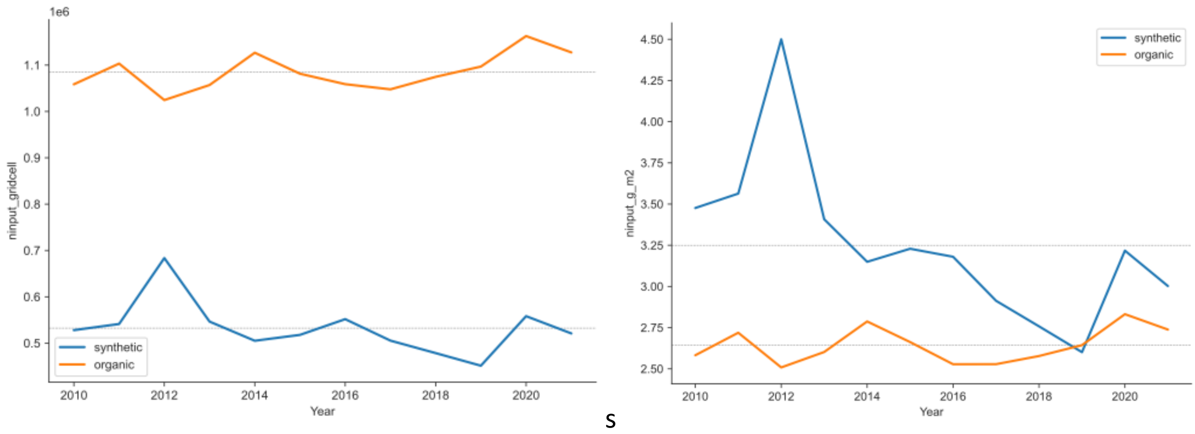

Figure 15a. Synthetic and organic fertiliser inputs over time, as prepared by ISPRA. Left: Total annual N inputs for Italy (Mt yr^{-1}). Right: Mean annual inputs (g-N yr^{-1} m^{-2} crop or grassland area).

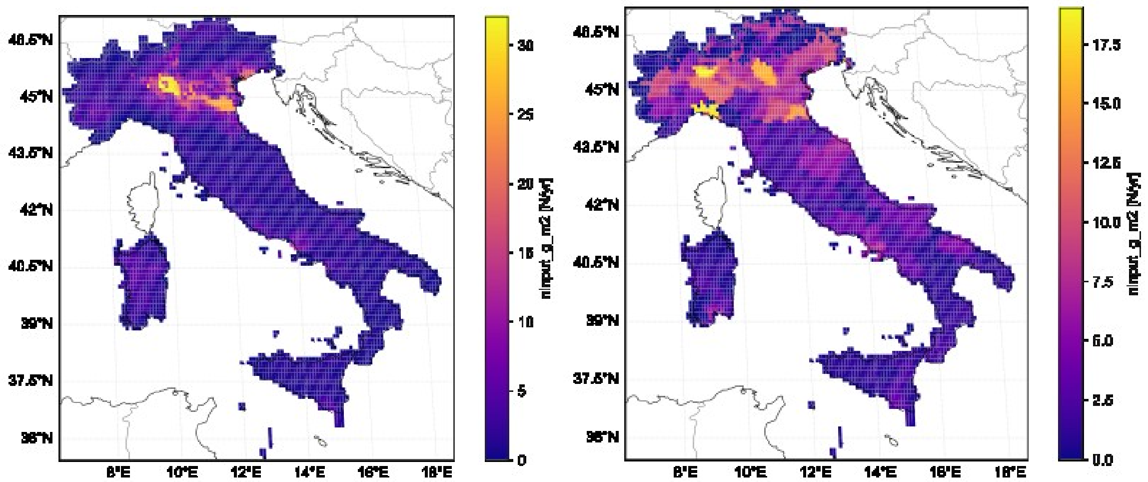

Figure 15b. Mean annual N inputs per grid cell in native resolution (0.1°) provided by ISPRA (g-N yr^{-1} m^{-2} grass/cropland area): organic (left) and synthetic (right) fertilisers.

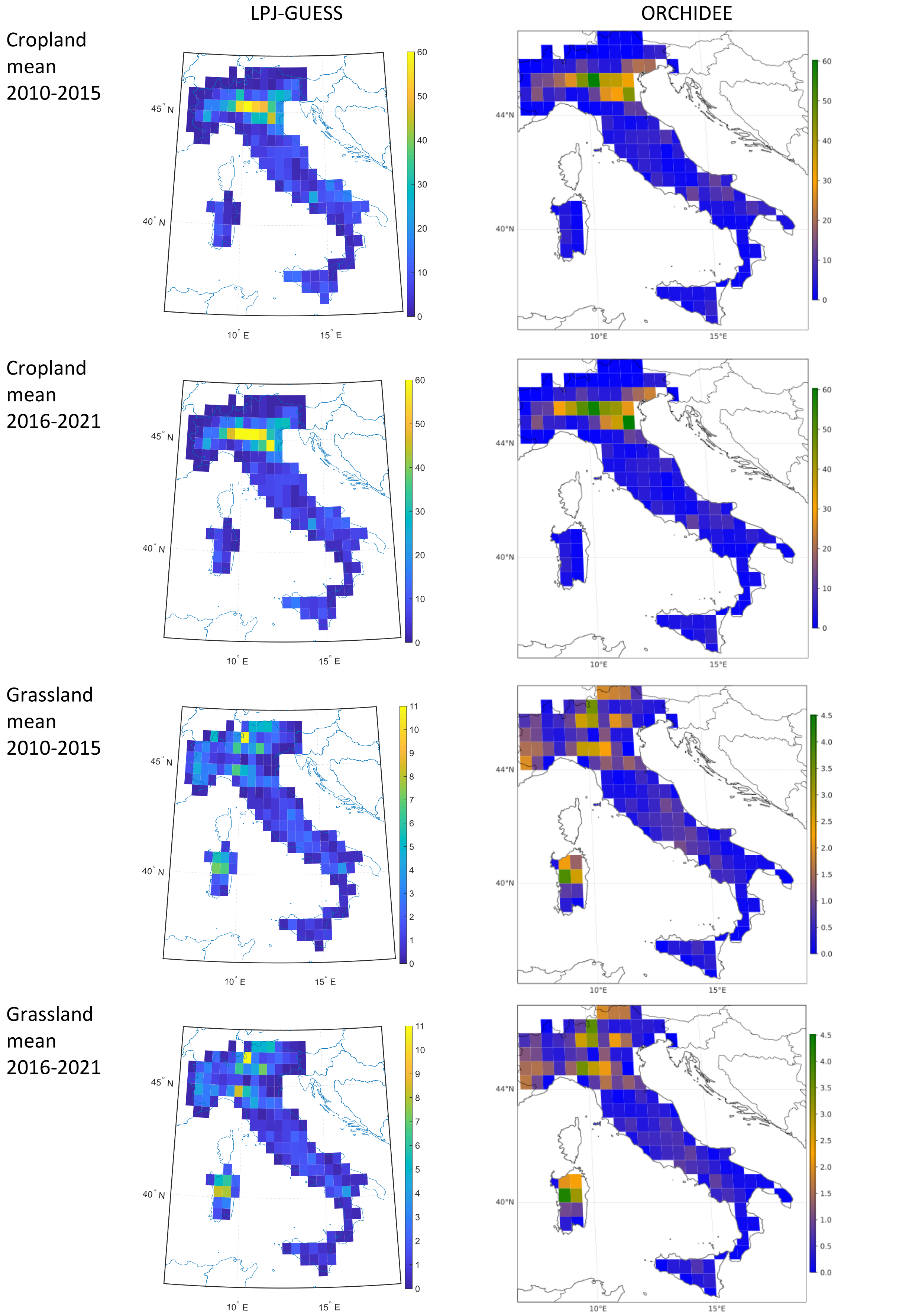

Figure 16. Organic and synthetic fertiliser inputs onto cropland and grassland soils re-gridded at 0.5° (Gg N grid^{-1} yr^{-1}).

In the simulations performed, atmospheric N deposition was taken from Tian et al. 2018 for ORCHIDEE and Lamarque et al. 2011 for LPJ-GUESS (see paragraphs 2.5.4 and 2.3 respectively) and includes deposition from anthropogenic non-agricultural sources. A comparison was done among default deposition used in LPJ-GUESS and deposition used in the inventory for the estimation of indirect N_2O emissions (only deposition from agricultural sources). Including N deposition from non-agricultural sources, recorded as memo item in the Italian inventory (Table 6 of CRF), total average deposition per hectare per year calculated for the Italian inventory is comparable with the default value used in LPJ-GUESS; however indirect N_2O emissions contained in WP2.2 priors include only deposition from agricultural source, so we can expect higher emissions from deposition simulated by models.

2010	2011	2012	2013	2014	2015	2016	2017	2018	2019	2020	2021
N deposition from other sectors - t N (from Table 6 of CRF 2023)											
299,727	288,273	276,182	245,636	239,909	227,818	224,000	219,545	209,364	203,636	182,000	192,818
N deposition from agriculture - t N (from Table 3.D CRF 2023)											
121,516	125,117	142,565	130,485	124,965	124,730	133,515	128,240	122,551	123,812	137,610	130,680
Total N deposition italian inventory kg N*ha-1*y-1											
13.95	13.69	13.86	12.45	12.08	11.67	11.84	11.51	10.99	10.84	10.58	10.71
Total N deposition LPJ-GUESS (kg N*ha-1*y-1)											
14.19	14.19	14.19	14.19	14.19	14.19	14.19	14.19	14.19	14.19	13.85	

Table 3. Comparison of default N deposition used in LPJ-GUESS simulation and estimated in the inventory.

4.2 N_2O emissions

Total N_2O emissions arising from cropland and grassland estimated in WP 2.2 priors for the years 2010-2021, based on Italian inventory submission 2023 ranged from 27 to 30.5 kt N_2O $year^{-1}$ (Table 4). A slight increasing trend 2010-2021 can be noted and a low interannual variability (Fig. 17).

Emissions simulated with LPJ-GUESS ranged from 17 to 31 kt N_2O $year^{-1}$ for grassland, and from 8 to 13 kt N_2O $year^{-1}$ for cropland respectively, resulting in total emissions of 25- 44 kt N_2O $year^{-1}$ during the simulated period (Table 4, Fig. 18). A slight increasing trend for cropland can be noted, more marked for grassland, and a higher interannual variability for grassland. N input to grassland used in LPJ-GUESS simulations of Natural Fluxes described in chapter 4 of deliverable 2.2(in Fig. 18 referred to as "Grass D2.2") and nitrogen transformation ("Ntrans") include only N inputs typical of pastures (urine and dung deposited by grazing animals) and atmospheric deposition, and are therefore much lower than in the inventory data.

Emissions simulated with ORCHIDEE ranged from 5 to 7.5 kt N_2O $year^{-1}$ for grassland, and from 6 to 14 kt N_2O $year^{-1}$ for cropland, respectivley, resulting in total emissions of 11-21.5 kt N_2O $year^{-1}$ during the simulated period. A slight increasing trend for grassland can be noted, more marked for cropland, and a higher interannual variability for cropland. In the re-gridding of the 0.1° land use data from ISPRA onto the 0.25° land use mask used by ORCHIDEE, approximately 14% of cropland and grassland area was lost. This had a minor impact on results expressed per hectare (Fig. 20), but led to an underestimation of results that are expressed per grid cell (Fig 21) and in the national total (Table 4 and Fig. 19). Future efforts can be made to negate and rectify this error. Even when increasing total ORCHIDEE N_2O emissions results by 14% they are still lower than WP2.2 priors and LPJ-GUESS emissions, but overall the total simulated N_2O emissions are on the same magnitude as those reported by WP2.2 priors (Fig. 17-19, 1000 tonnes = 1 Gg).

Table 4. Range of simulated N_2O emissions (direct+indirect from atmospheric deposition) for the period 2010-2021, compared with WP 2.2 priors

	CROPLAND	GRASSLAND	TOTAL
WP 2.2 priors from IT Inventory 2023 (2010-2021)			27-30.5 kt N_2O $year^{-1}$
LPJ-GUESS simulation 2010-2021	8-13 kt N_2O $year^{-1}$	17-31 kt N_2O $year^{-1}$	25-44 kt N_2O $year^{-1}$
ORCHIDEE simulation 2010-2021	6-14 kt N_2O $year^{-1}$	5-7.5 kt N_2O $year^{-1}$	11-21.5 kt N_2O $year^{-1}$

The simulated emissions from the cropland area are comparable for the two models. The simulated increasing trend for the cropland-grassland area is stronger than in the WP2.2 priors data. For the grassland area the LPJ-GUESS results show almost twice as high emissions than from the cropland, though the total area is 65% less and it only receives organic fertiliser. One of the reasons can be that the grassland area is simulated as pastures, and 62.5% of the nitrogen contained in grasses is directly returned to ecosystem by the model, with a probable double counting of nitrogen input from grazing animals, also contained in ISPRA N organic input (see par. 2.5.4). ORCHIDEE simulations result in higher emissions for cropland than grassland using ISPRA N input (Figure 19). However, Figure 20 shows that also the ORCHIDEE model has substantially higher grassland emissions per unit area: no harvest is assumed on the grassland area for ORCHIDEE (Figure 24). Moreover, both models internally calculate N input from crop residues of precedent crops (soil and litter in ORCHIDEE), so there probably was a double counting of N input from crop residues too.

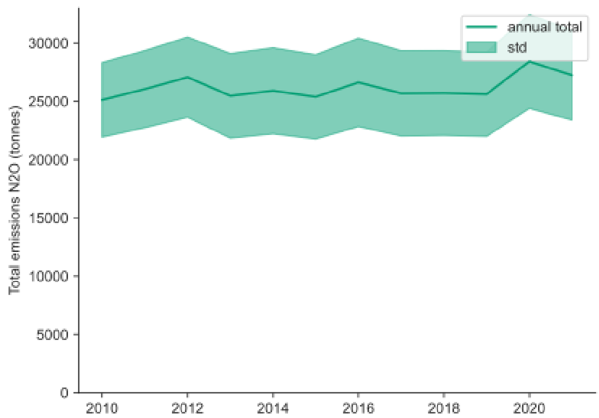

Figure 17. Annual direct N_2O emissions for Italy, as estimated for WP2.2 priors, starting from inventory submission 2023

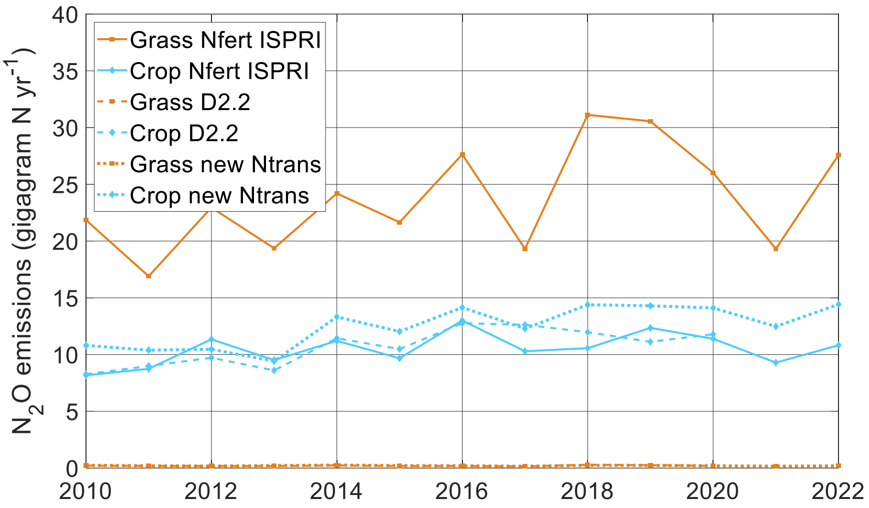

Figure 18. Total N_2O flux for Italy from cropland and grassland soils 2010-2022 simulated by LPJ-GUESS. A comparison is made against the results from the Avengers D2.1 deliverable using CMIP6 fertilisation amounts (D2.2 in legend) and a complementary run using new code for N transformations.

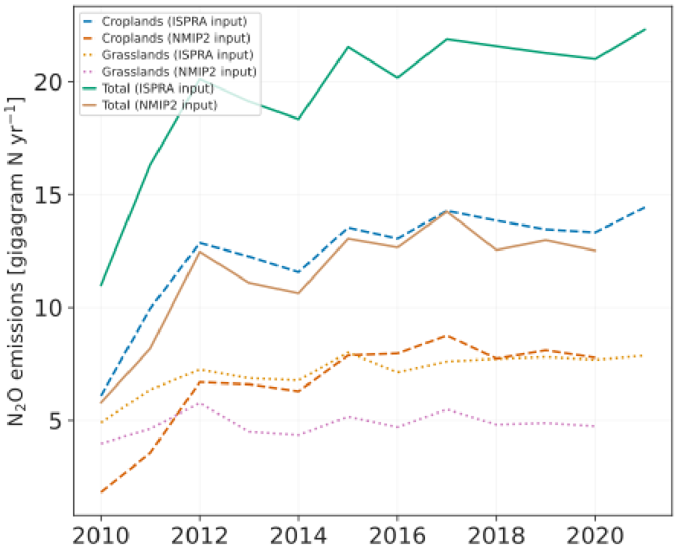

Figure 19. Annual N_2O emissions for Italy comparing the effects of using nitrogen inputs prepared by ISPRA and the NMIP2 product on simulated ORCHIDEE emissions.

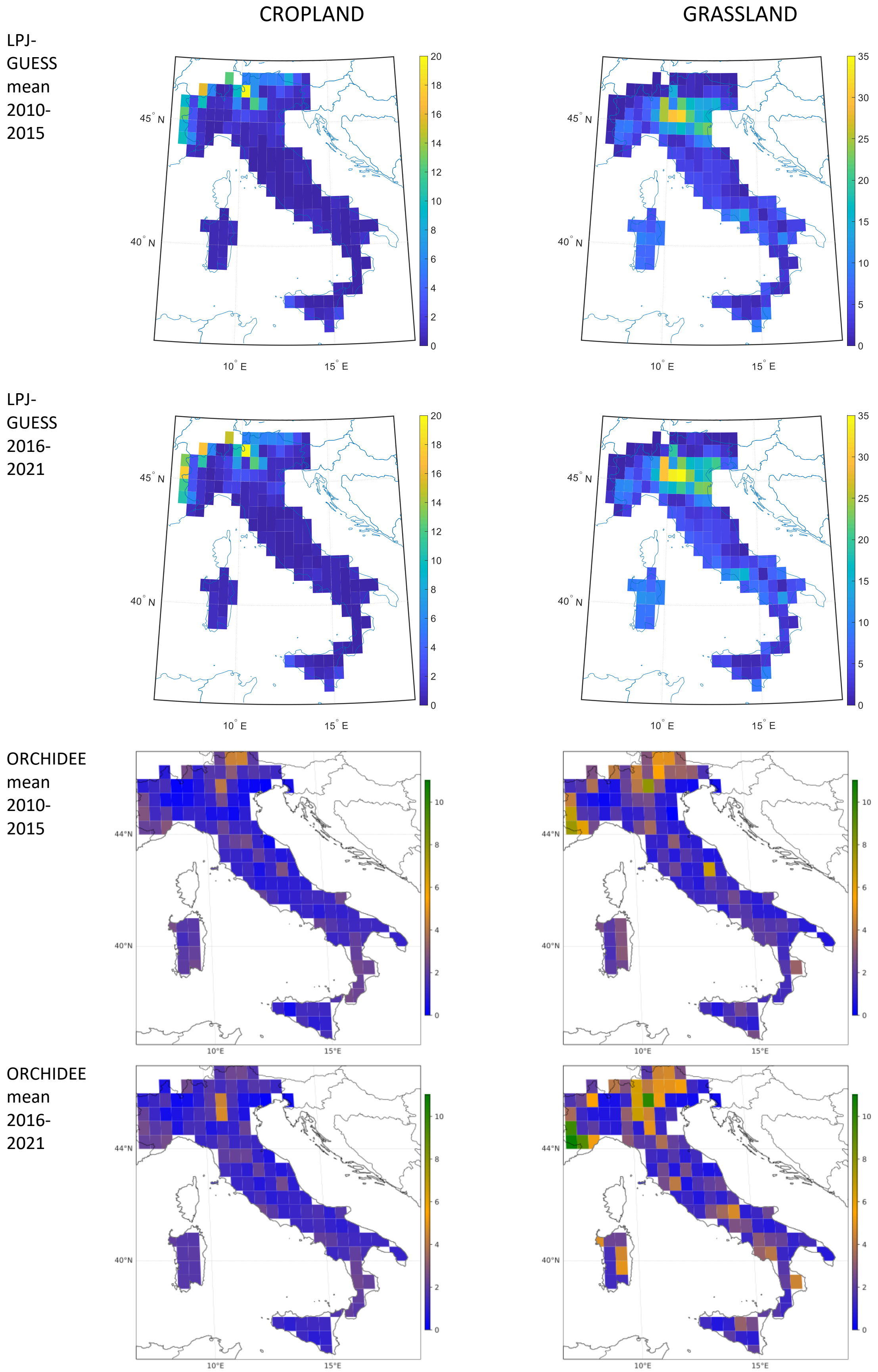

Figure 20. Simulated yearly mean N_2O flux from cropland and grassland soils per unit cropland/grass area (kg N-N_2O ha^{-1} yr^{-1}).

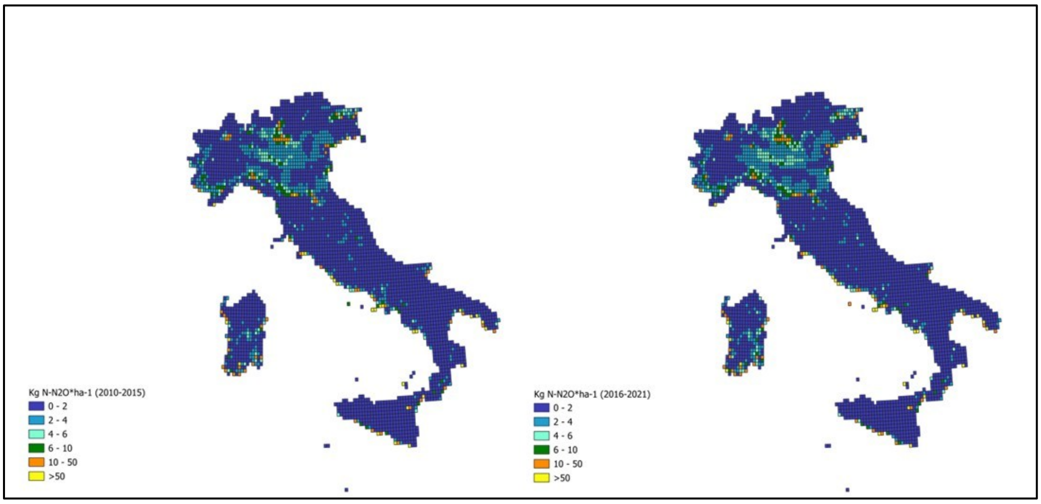

Figure 21. Yearly mean N_2O flux per unit cropland + grassland area estimated at 0.1° grid-cell in WP2.2 priors starting from inventory submission 2023 (kg N-N_2O $ha^{-1}yr^{-1}$).

The simulated yearly emissions per hectare for the most of the Italian cropland and grassland area are in the range 0-15 kg N-N_2O ha^{-1} yr^{-1} for LPJ-GUESS and 0-3 kg N-N_2O ha^{-1} yr^{-1} for ORCHIDEE; for the hotspot of the Po river plain region simulations are in the range 20-35 kg N-N_2O ha^{-1} yr^{-1} and 4-10 kg N-N_2O ha^{-1} yr^{-1} for LPJ-GUESS and ORCHIDEE respectively (Fig. 20). The hotspots of the emissions (Fig. 20) are associated with higher nitrogen input (Fig. 16). The N_2O fluxes per unit of cropland and grassland area showed in Fig. 21 were estimated dividing the gridded WP2.2 priors emissions by the surface of CLC cropland and grassland per grid cell: for the most of the Italian cropland and grassland estimates are in the range 0-2 kg N-N_2O ha^{-1} yr^{-1}, while for the Po Plain region 2-6 kg N-N_2O ha^{-1} yr^{-1} were estimated with some grid cells peaking up to 10-50 kg N-N_2O ha^{-1} yr^{-1}; 1% of the cells across the entire Country exceed the 50 kg N ha^{-1} yr^{-1}.

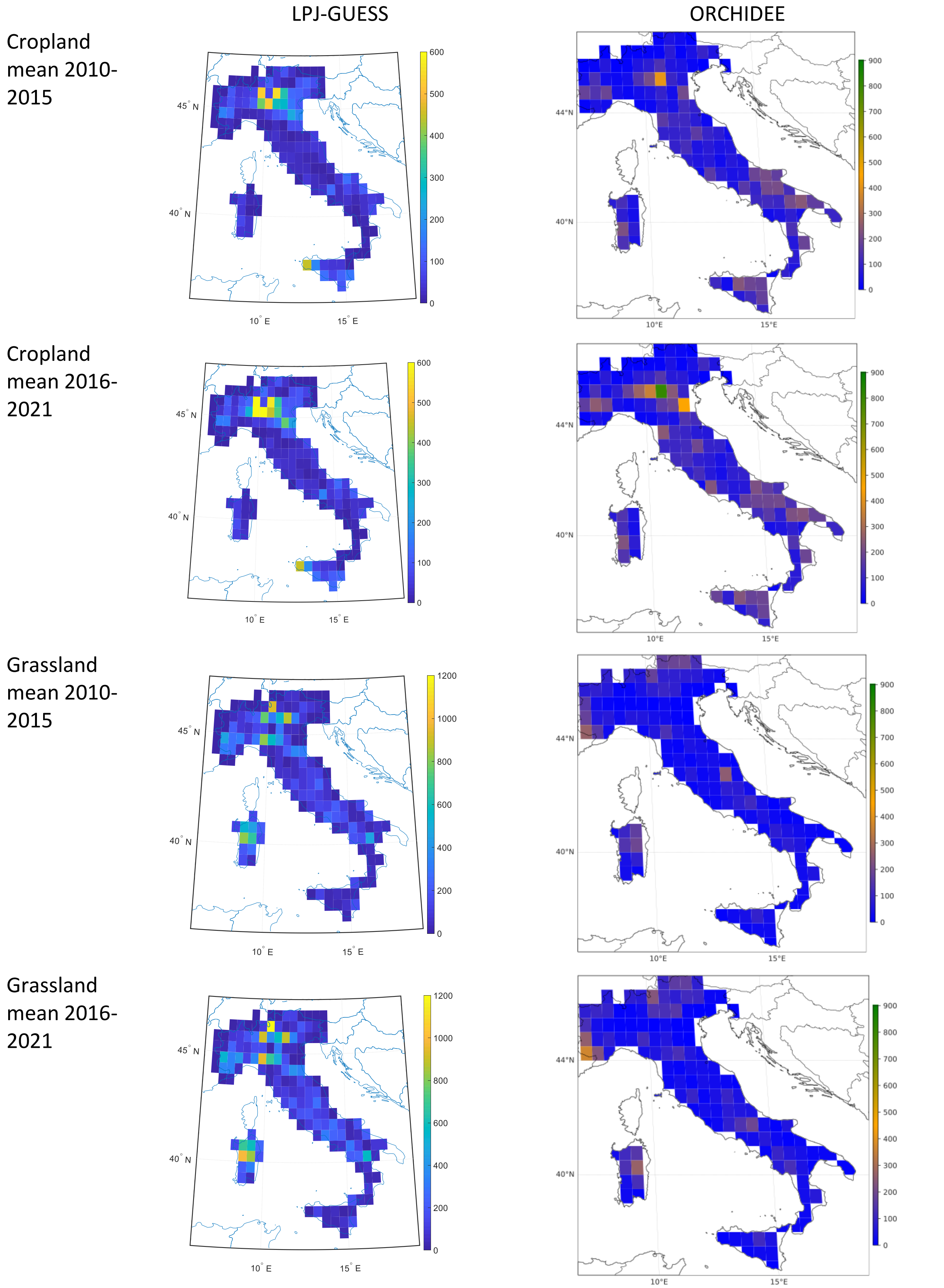

Figure 21. Simulated total N_2O flux from cropland and grassland 0.5° grid-cell areas (tonne N-N_2O gridcell^{-1} yr^{-1}).

4.3 N_2O emission factors

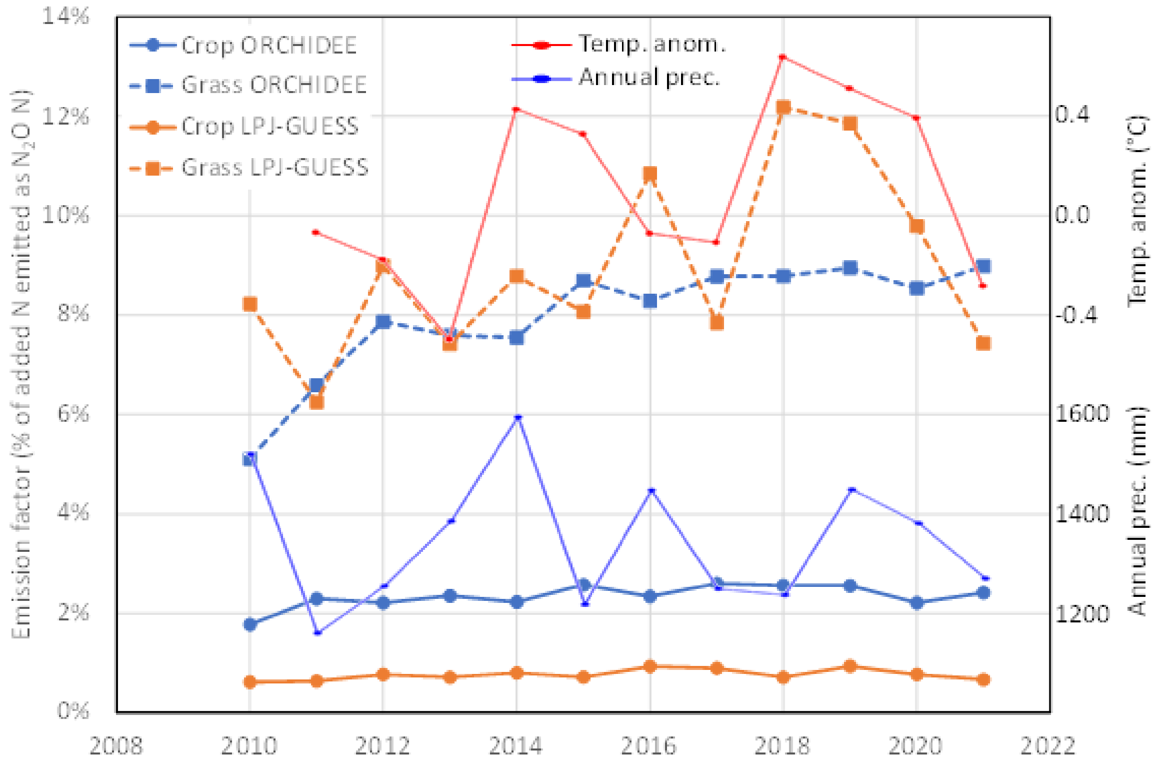

Figure 22. Simulated national level N_2O emission factors from cropland and grassland soils 2010-2022 (% of added N emitted as N_2O-N) compared to the anomalies of mean annual temperature and mean total precipitation for Italy.

The implied emission factors for direct N_2O emissions used for Italy in inventory submission 2023 were 0.96% for mineral and 1.0% for organic fertilisers (see Table 1); including also indirect emissions from deposition, the overall implied emission factor used by the Italian inventory in 2023 is 1.36%; it falls between the values obtained from the two models for what concern cropland (Fig. 22). The IPCC Tier 1 EF for direct N_2O emissions as updated by refinement 2019 (IPCC, 2019) are 0.5% for dry climates (uncertainty range 0 - 1,1%), and for wet climates, 1.6% for mineral fertilizers uncertainty range 1.3 - 1.9%) and 0.6% for organic fertilizers (uncertainty range 0.1 - 1.1%). The simulated emission factors for grassland are an order of magnitude too high for both models, indicating that a refinement of those simulations is needed before they can be used quantitively. Most likely this can be attributed to an inappropriate representation of grassland ecosystem in the models. Even if the simulated EF are not readily usable, the simulated annual variations and temporal trends, related to temperature anomalies and total annual precipitation, most clearly seen in the simulated grassland factor for LPJ-GUESS, constitute relevant information potentially usablefor future improvement of EF within the inventory (Fig. 22). The annual variability of EF simulated by LPJ-GUESS for grassland seems to be influenced not only by precipitations, but also by temperature.

A reason for the lower simulated emission factor for cropland in LPJ-GUESS than in ORCHIDEE can be that irrigation is applied to a fraction of the land, as specified by the CMIP6 setup data. A preliminary test without irrigation resulted in a higher factor. In the reality irrigation is largely used in Italy, so this aspect could be improved too in future simulations, trying to validated simulated yields.

In the following figure it can be appreciated the spatial variability of EF. The areal distributions of the emission factor show some hot areas in the north and for ORCHIDEE also in South for the cropland area (Fig. 23). For grassland the areas with high emission factors have a larger distribution over most part of the country.. For what concern mineral fertilizers distributed on cropland there could be a misalignment among the amount of N input and the cropland surface in a certain province(activity data used in the inventory is the amount sold at NUTS3 level); it also affect simulated EF.

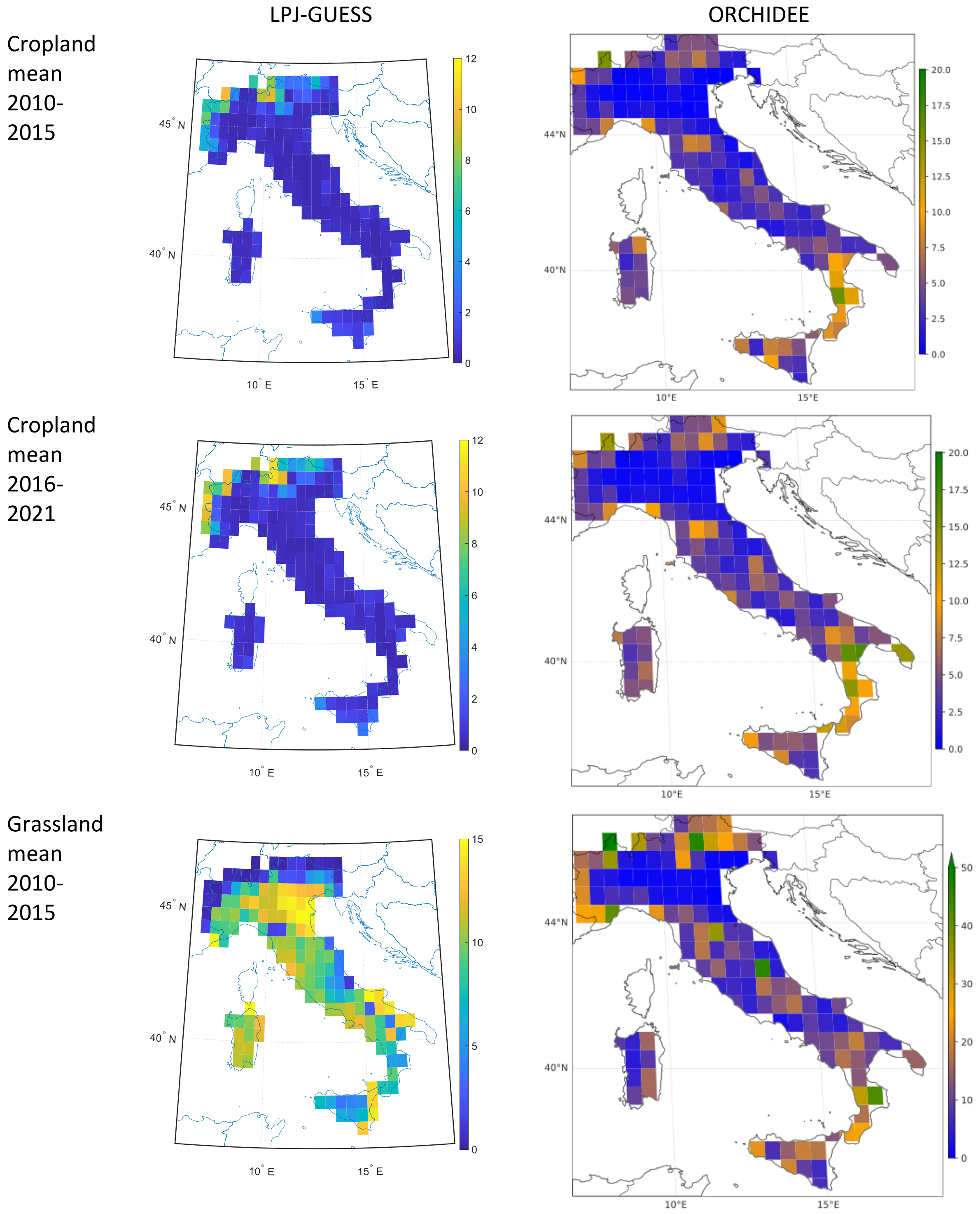

Grassland mean 2016-2021

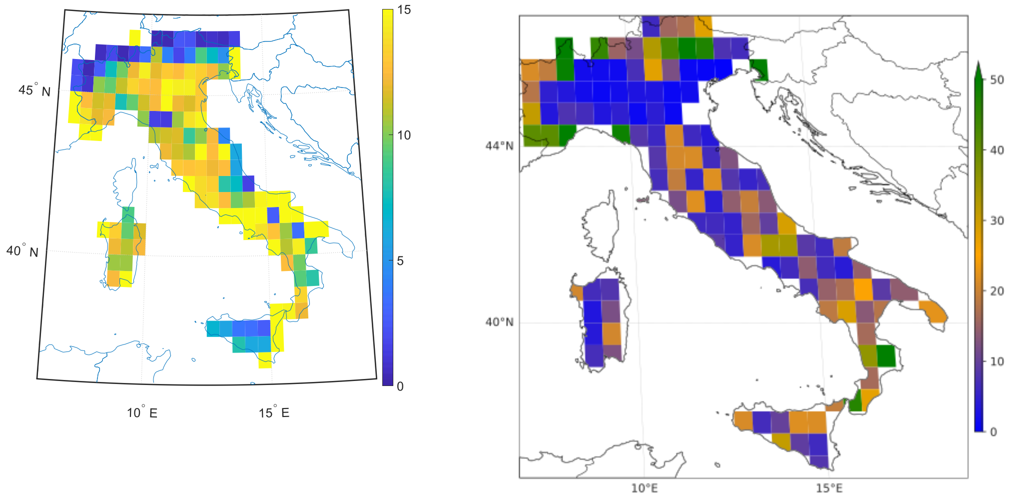

Figure 23. Simulated N_2O emission factors from cropland and grassland soils (% of added N emitted as N_2O-N).

4.4 Total N balance

The total N balance of the land shows some distinct differences both between models and within models for cropland and grassland, respectively (Fig. 24). Harvest removes a very large fraction of the added N in the LPJ-GUESS cropland simulations, while it is a smaller fraction in ORCHIDEE cropland simulations, even smaller in the LPJ-GUESS grassland simulations and zero in ORCHIDEE grassland simulations where grasslands are not harvested (discussed further in Sect. 5.2). Leaching is a rather large component in the grassland simulations, while it is a small fraction for cropland. The N lost in leaching, expressed as percentage of N added through fertilization is assumed as 24% in IPCC GL (table 2); LPJ-GUESS simulation resulted in about 10% for cropland and about 50% for grassland; ORCHIDEE simulation resulted in about 5% for cropland and between 22% and 44% for grassland.

The soil and litter pools in both models collect and store nitrogen that is not lost to harvest, leaching or emitted to the atmosphere. A calibration and validation of N lost through harvest is needed.

In Fig. 24 it can be noted how in ORCHIDEE simulations a lower amount of N input from fertilization was considered, due to the error described in paragraph 4.2.

LPJ-GUESS Cropland

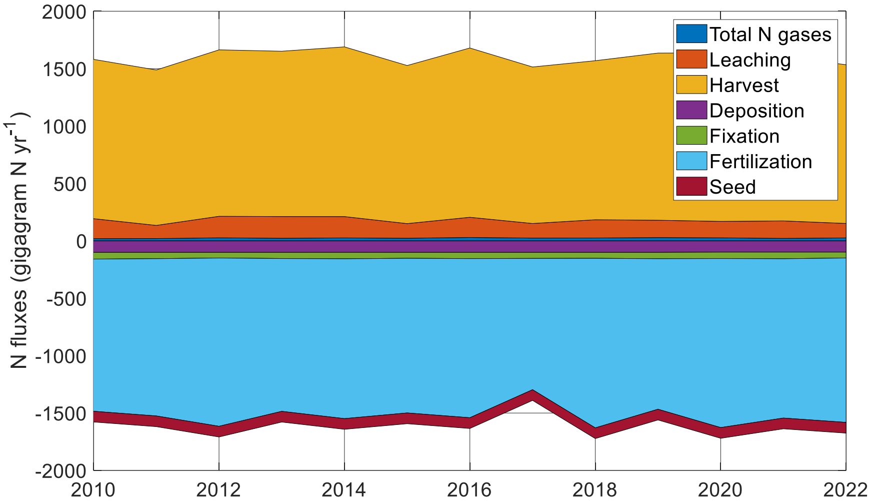

LPJ-GUESS Grassland

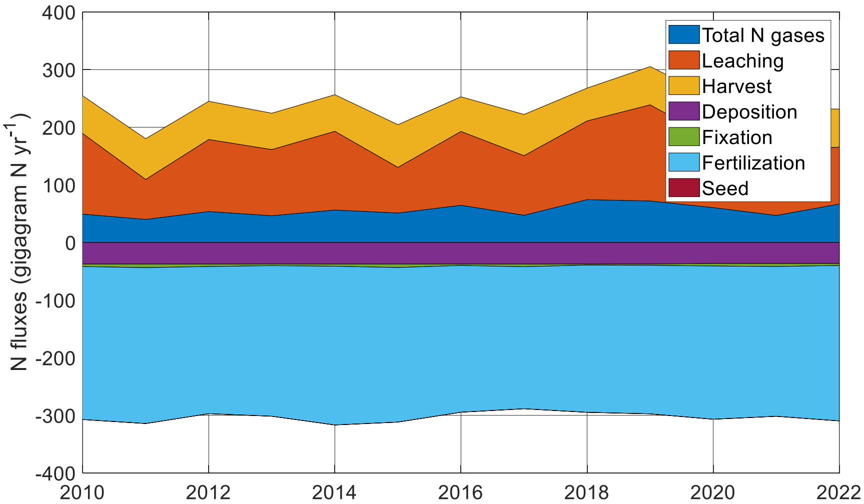

ORCHIDEE Cropland

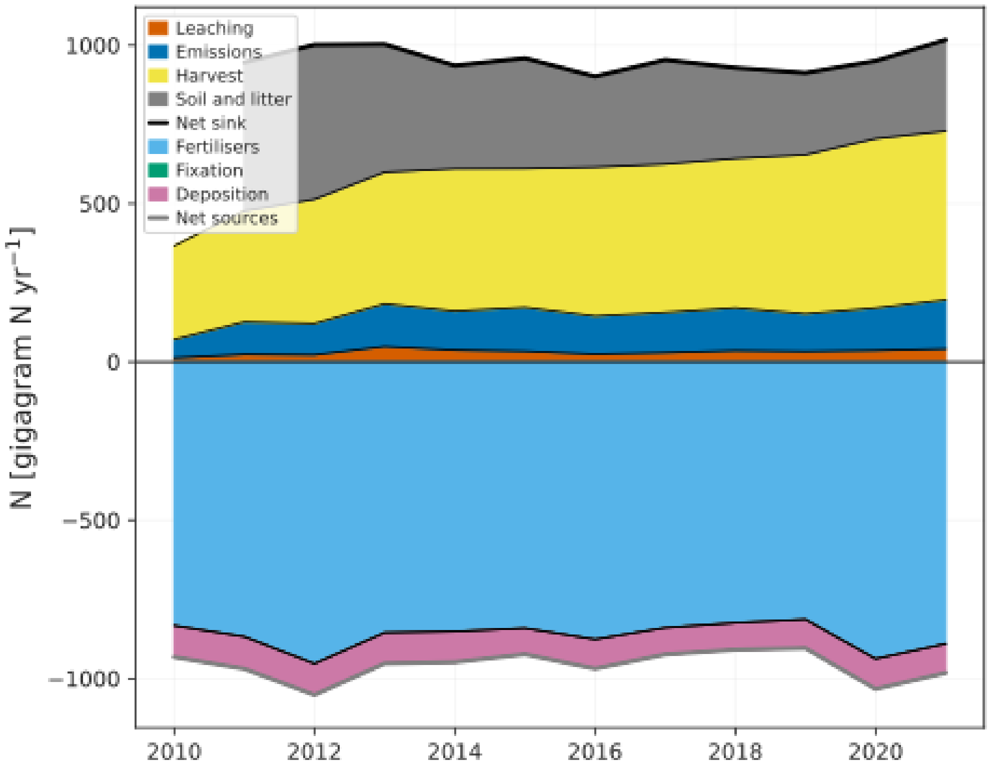

ORCHIDEE
Grassland

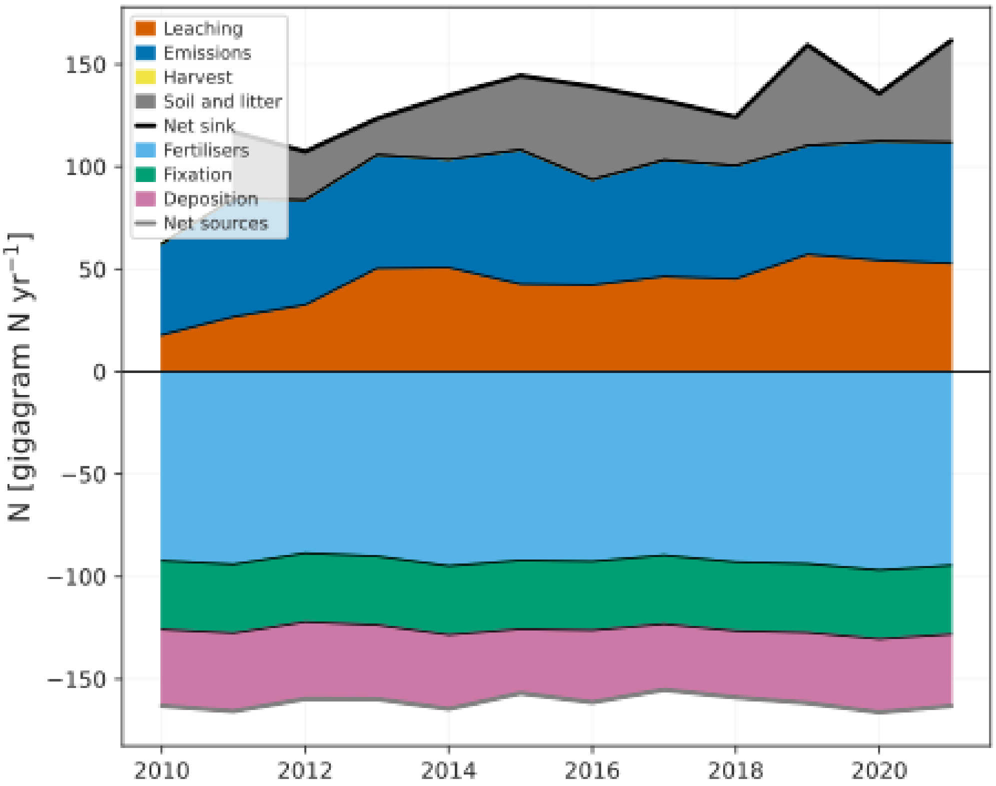

Figure 24. Total simulated N balance from cropland and grassland 2010-2022.

5 Key messages

Our model simulations demonstrated the usefulness of DGVMs for estimating spatial and temporal changes in carbon stocks (forests in Sweden) and N_2O emissions (agriculture in Italy). In both cases the simulations supported the hypothesis that using a constant emission factor is an oversimplification. Incorporating information on the influence of weather events, climate extremes and different management methods can lead to more accurate assessments. However, the model comparison also showed the significant impact of uncertainties in model parameterization, highlighting the need for further model development, calibration, and evaluation.

5.1 Lessons from the forest case study

- **Forest age, age structure and harvest levels are important drivers of variation in emissions/uptake over time.** According to the simulations, longer rotation periods would lead to increased carbon uptake. The carbon uptake/emission factor is sensitive to settings that affect age and harvest levels, e.g. rotation period length and initiated age structure. The two DGVMs used different strategies to create a model setup that best matches the inventory data, while more sophisticated methods are still being developed.

- **There is considerable annual variation in simulated emissions/uptake from the Swedish forest, especially when analysed at a higher spatial resolution than the national level.** Drought is a key factor contributing to this annual variation.
- **Different forest types or plant functional types show significant differences in simulated emissions/uptake.** However, there is substantial uncertainty regarding how accurately the models represent the true differences between species and plant functional types.

5.2 Lessons from the agricultural case study

- **Simulated EFs from grassland areas are much higher than the one reported by the inventory. This discrepancy is mainly due to the simplified representation of these complex systems in both models (e.g. regarding grazing, hey harvest and fertilizer input).** A key difference between the cropland and grassland simulations is that, in cropland, a very high fraction of nitrogen input ends up in the harvested biomass when considering the total nitrogen balance. In contrast, LPJ-GUESS simulates a smaller harvested fraction for grasslands, and ORCHIDEE assumes no harvest at all. However, the increasing trend of simulated EF and its interannual variability (6% - 12% for LPJ-GUESS and 5% - 9% for ORCHIDEE simulation) is something relevant to be further investigated, in order to understand the need of a possible methodology improvement to consider the influence of meteorological variability in the inventory estimates. ORCHIDEE does not have pastures. In this study we made a first step to simulate grasslands as pastures by adding organic fertilisers to grasslands. We see higher emissions factors from grasslands because nitrogen is not being removed by grazing and/or harvest as is typical of a pasture. Next steps are to include harvest or grazing of grasslands to increase realism and improve reliability of nitrogen emissions from grasslands in ORCHIDEE.
- **For cropland, simulated emission factors are comparable to emission factor used in Italy's reporting, but does not add relevant information to improve it.**
- Nitrogen deposition used in simulation is almost double of the one considered in the inventory for the estimate of indirect N_2O emissions (only from agricultural sources).
- A possible double counting occurred in the simulations is due to the inclusion of N input from crop residues (which is the third source of N input in the inventory after mineral fertilizers and manure) within organic N input. In fact both the models calculate internally N input from crop residues and add it to the next crop cycle. Another possible double counting is for grassland the N input from urine and dung deposited by grazing animals for LPJ-GUESS
- **Further calibration and validation of yield and nitrogen harvested is necessary for both modelling exercises, considering irrigated and non-irrigated areas.** In ORCHIDEE simulations an error in re-gridding cropland and grassland area occurred (14% underestimated), which led to lower N input used for modelling. LPJ-GUESS simulated emissions are currently comparable with the reported emissions in the inventory, however, nitrogen inputs are higher because of N depositions and double counting of N input from grazing animals and crop residues, which could mean that inventory N_2O emissions are in general overestimated.

6 References

Batjes, N. H. 2005: ISRICE-WISE global data set of derived soil properties on a 0.5 by 0.5 degree grid (version 3.9), Report 08 ISRIC World Soil Information, Wageningen, the Netherlands.

Bellassen, V., Le Maire, G., Dhôte, J. F., Ciais, P., and Viovy, N. 2010: Modelling forest management within a global vegetation model—Part 1: Model structure and general behaviour. Ecological Modelling, 221(20), 2458–2474. https://doi.org/https://doi.org/10.1016/j.ecolmodel.2010.07.008

Frieler, K., Volkholz, J., Lange, S., Schewe, J., Mengel, M., Del Rocío Rivas López, M., Otto, C., Reyer, C. P. O., Karger, D. N., Malle, J. T., Treu, S., Menz, C., Blanchard, J. L., Harrison, C. S., Petrik, C. M., Eddy, T. D., Ortega-Cisneros, K., Novaglio, C., Rousseau, Y., … Bechtold, M. (2024). Scenario setup and forcing data for impact model evaluation and impact attribution within the third round of the Inter-Sectoral Impact Model Intercomparison Project (ISIMIP3a). Geoscientific Model Development, 17(1), 1–51. https://doi.org/10.5194/gmd-17-1-2024

Grelle, A., Hedwall, P. O., Strömgren, M., Håkansson, C., and Bergh, J. 2023: From source to sink-recovery of the carbon balance in young forests. Agricultural and Forest Meteorology, 330, Article 109290. https://doi.org/10.1016/j.agrformet.2022.109290.

Hickler, T., Vohland, K., Feehan, J., Miller, P. A., Smith, B., Costa, L.,…Sykes, M. T. 2012: Projecting the future distribution of European potential natural vegetation zones with a generalized, tree species-based dynamic vegetation model. Global Ecology and Biogeography, 21, 50-63, https://doi.org/10.1111/j.1466-8238.2010.00613.x.

Hurtt, G. C., Chini, L., Sahajpal, R., Frolking, S., Bodirsky, B. L., Calvin, K.,…Zhang, X. 2020: Harmonization of global land use change and management for the period 850–2100 (LUH2) for CMIP6. Geosci. Model Dev., 13, 5425-5464, https://doi.org/10.5194/gmd-13-5425-2020.

IPCC 2006: 2006 IPCC Guidelines for National Greenhouse Gas Inventories, Prepared by the National Greenhouse Gas Inventories Programme, Eggleston H.S., Buendia L., Miwa K., Ngara T. and Tanabe K. (eds). Published: IGES, Japan. ISBN 4-88788-032-4

IPCC 2019: 2019 Refinement to the 2006 IPCC Guidelines for National Greenhouse Gas Inventories, Calvo Buendia, E., Tanabe, K., Kranjc, A., Baasansuren, J., Fukuda, M., Ngarize S., Osako, A., Pyrozhenko, Y., Shermanau, P. and Federici, S. (eds). Published: IPCC, Switzerland. ISBN 978-4-88788-232-4

Jönsson, A. M., Schroeder, L. M., Lagergren, F., Anderbrant, O., and Smith, B. 2012: Guess the impact of Ips typographus - An ecosystem modelling approach for simulating spruce bark beetle outbreaks, Agricultural and Forest Meteorology, 166-167, 188-200, https://doi.org/10.1016/j.agrformet.2012.07.012.
Krinner, G., Viovy, N., de Noblet-Ducoudré, N., Ogée, J., Polcher, J., Friedlingstein, P., Ciais, P., Sitch, S., and Prentice, I. C. (2005). A dynamic global vegetation model for studies of the coupled atmosphere-biosphere system. Global Biogeochemical Cycles, 19(1), 1–33. https://doi.org/10.1029/2003GB002199

Lagergren, F., Jönsson, A. M., Blennow, K., and Smith, B. 2012: Implementing storm damage in a dynamic vegetation model for regional applications in Sweden, Ecological Modelling, 247, 71-82, https://doi.org/10.1016/j.ecolmodel.2012.08.011.

Lagergren, F., Jönsson, A. M., Lindeskog, M., and Pugh, T. A. M. 2025: Combining empirical and mechanistic understanding of spruce bark beetle outbreak dynamics in the LPJ-GUESS (v4.1, r13130) vegetation model. Geoscientific Model Development, 18, 8071–8090. https://doi.org/10.5194/gmd-18-8071-2025.

Lamarque, J.-F., Kyle, G. P., Meinshausen, M., Riahi, K., Smith, S. J., van Vuuren, D. P., Conley, A. J., and Vitt, F., 2011: Global and regional evolution of short-lived radiatively-active gases and aerosols in the Representative concentration Pathways, Climatic Change, 109, 191–212, 2011. https://doi.org/10.1007/s10584-011-0155-0

Le Quéré, C., Andrew, R. M., Friedlingstein, P., Sitch, S., Hauck, J., Pongratz, J., Pickers, P. A., Korsbakken, J. I., Peters, G. P., Canadell, J. G., Arneth, A., Arora, V. K., Barbero, L., Bastos, A., Bopp, L., Chevallier, F., Chini, L. P., Ciais, P., Doney, S. C., … Zheng, B. 2018: Global Carbon Budget 2018. Earth System Science Data, 10(4), 2141–2194. https://doi.org/10.5194/essd-10-2141-2018

Lindeskog, M., Smith, B., Lagergren, F., Sycheva, E., Ficko, A., Pretzsch, H., and Rammig, A. 2021: Accounting for forest management in the estimation of forest carbon balance using the dynamic vegetation model LPJ-GUESS (v4.0, r9710): implementation and evaluation of simulations for Europe, Geoscientific Model Development, 14, 6071-6112, https://doi.org/10.5194/gmd-14-6071-2021.

Lindroth, A., Lagergren, F., Grelle, A., Klemedtsson, L., Langvall, O., Weslien, P., and Tuulik, J. 2009: Storms can cause Europe-wide reduction in carbon sink. Global Change Biology, 15(2), 346-355. https://doi.org/10.1111/j.1365-2486.2008.01719.x.

Lindroth, A., Holst, J., Linderson, M.-L., Aurela, M., Biermann, T., Heliasz, M.,…Nilsson, M. 2020: Effects of drought and meteorological forcing on carbon and water fluxes in Nordic forests during the dry summer of 2018. Philosophical Transactions of the Royal Society B-Biological Sciences, 375, Article 20190516. https://doi.org/10.1098/rstb.2019.0516.

Ma, J. Y., Arneth, A., Smith, B., Anthoni, P., Xu, R., Eliasson, P.,…Olin, S. 2025: Soil nitrous oxide emissions from global land ecosystems and their drivers within the LPJ-GUESS model (v4.1). Geoscientific Model Development, 18, 3131-3155. https://doi.org/10.5194/gmd-18-3131-2025.

Marini, L., Økland, B., Jönsson, A. M., Bentz, B., Carroll, A., Forster, B.,…Schroeder, M. 2017: Climate drivers of bark beetle outbreak dynamics in Norway spruce forests. Ecography, 40, 1426-1435. https://doi.org/10.1111/ecog.02769.

Naudts, K., Ryder, J., McGrath, M. J., Otto, J., Chen, Y., Valade, A., Bellasen, V., Berhongaray, G., Bönisch, G., Campioli, M., Ghattas, J., De Groote, T., Haverd, V., Kattge, J., MacBean, N., Maignan, F., Merilä, P., Penuelas, J., Peylin, P., … Luyssaert, S. 2015: A vertically discretised canopy description for ORCHIDEE (SVN r2290) and the modifications to the energy, water and carbon fluxes. Geoscientific Model Development, 8(7), 2035–2065. https://doi.org/10.5194/gmd-8-2035-2015Olin, S., Lindeskog, M., Pugh, T. A. M., Schurgers, G., Wårlind, D., Mishurov, M.,…Arneth, A. 2015: Soil carbon management in large-scale Earth system modelling: implications for crop yields and nitrogen leaching. Earth System Dynamics, 6, 745-768. https://doi.org/10.5194/esd-6-745-2015.

Pucher, C., Neumann, M., and Hasenauer, H. 2022: An Improved Forest Structure Data Set for Europe. Remote Sensing, 14(395). https://doi.org/10.3390/rs14020395.

Romano, D., Arcarese, C., Bernetti, A., Caputo, A., Cordella, M., De Lauretis, R., Di Cristofaro, E., Gagna, A., Gonella, B., Moricci, F., Pellis, G., Taurino, E., Vitullo, M., 2023: Italian Greenhouse Gas Inventory 1990-2021 National Inventory Report 2023. ISPRA, Rapporti 383/2023. ISBN 978-88-448-1155-6

Siebert, S., Döll, P., Hoogeveen, J., Faures, J. M., Frenken, K., and Feick, S. 2005: Development and validation of the global map of irrigation areas. Hydrology and Earth System Sciences, 9(5), 535–547. https://doi.org/10.5194/hess-9-535-2005

Smith, B., Prentice, I.C. and Sykes, M.T. 2001: Representation of vegetation dynamics in the modelling of terrestrial ecosystems: comparing two contrasting approaches within European climate space. Global Ecology and Biogeography: 621-637. https://doi.org/10.1046/j.1466-822X.2001.00256.x.

Smith, B., Wårlind, D., Arneth, A., Hickler, T., Leadley, P., Siltberg, J., and Zaehle, S. 2014: Implications of incorporating N cycling and N limitations on primary production in an individual-based dynamic vegetation model. Biogeosciences, 11(7): 2027-2054. https://doi.org/10.5194/bg-11-2027-2014.

Taurino, E., et al., 2022: La disaggregazione a livello provinciale dell'inventario nazionale delle emissioni. ISPRA, Rapporti 369/2022. ISBN 978-88-448-1123-5

Tian, H., Yang, J., Lu, C., Xu, R., Canadell, J. G., Jackson, R. B., Arneth, A., Chang, J., Chen, G., Ciais, P., Gerber, S., Ito, A., Huang, Y., Joos, F., Lienert, S., Messina, P., Olin, S., Pan, S., Peng, C., … Zhu, Q. 2018: The global N2O model intercomparison project. Bulletin of the American Meteorological Society, 99(6), 1231–1251. https://doi.org/10.1175/BAMS-D-17-0212.1

Tian, H., Bian, Z., Shi, H., Qin, X., Pan, N., Lu, C., Pan, S., Tubiello, F. N., Chang, J., Conchedda, G., Liu, J., Mueller, N., Nishina, K., Xu, R., Yang, J., You, L., and Zhang, B. 2022: History of anthropogenic Nitrogen inputs (HaNi) to the terrestrial biosphere: A 5arcmin resolution annual dataset from 1860 to 2019. Earth System Science Data, 14(10), 4551–4568. https://doi.org/10.5194/essd-14-4551-2022

Vuichard, N., Messina, P., Luyssaert, S., Guenet, B., Zaehle, S., Ghattas, J., Bastrikov, V., and Peylin, P. 2019: Accounting for carbon and nitrogen interactions in the global terrestrial ecosystem model ORCHIDEE (trunk version, rev 4999): multi-scale evaluation of gross primary production. Geoscientific Model Development, 12(11), 4751–4779. https://doi.org/10.5194/gmd-12-4751-2019

Wang, EL. and Engel, T. 1998: Simulation of phenological development of wheat crops. Agricultural Systems 58(1): 1-24 DOI10.1016/S0308-521X(98)00028-6

Zaehle, S., Friend, A. D., Friedlingstein, P., Dentener, F., Peylin, P., and Schulz, M. 2010: Carbon and nitrogen cycle dynamics in the O-CN land surface model: 2. Role of the nitrogen cycle in the historical terrestrial carbon balance. Global Biogeochemical Cycles, 24(1), 1–14. https://doi.org/10.1029/2009gb003522

Zaehle, S., and Friend, A. D. 2010: Carbon and nitrogen cycle dynamics in the O-CN land surface model: 1. Model description, site-scale evaluation, and sensitivity to parameter estimates. Global Biogeochemical Cycles, 24(1), 1–13. https://doi.org/10.1029/2009GB003521

Appendices

Annex I: Forestry in Sweden

Use of NFI data for the setup of the LPJ-GUESS simulations for Sweden

National forest inventory (NFI) data for the period 1988-1992 were used for initiating the forest conditions, with county data on seven forest types (*Pinus sylvestris* pine forest, *Pinus contorta* pine forest, Spruce forest, mixed needle-leafed forest, mixed forest dominated by broad-leafed species, Nemoral broadleafed forest and Boreal broadleafed forest) and twelve age-classes (0-2, 3-10, 11-20, 21-30, 31-40, 41-60, 61-80, 81-100, 101-120, 121-140, 141-160 and 161+ years). The forest type and age distribution data were translated to six species types with 10-year age classes, continuous forestry and unmanaged forest, managed with different rotation periods for different parts of the country (Figure 1). *P. Contorta* was included in the pine forest species class. For the inventoried 0-2 age class there was also an area reported for which no species class had been assigned as it had been recently harvested, this area was split between the species types in the same proportion as their share of the total 0-2 years area. For the inventoried age classes with a 20-year resolution (>40 years) the area was split equally between the two simulated 10-year classes. The area of continuous cover forestry was set to the sum of all species types areas for the 141-160 years age class in LPJ-GUESS groups 1-2 and to the 121-140 age-class area in group 3-5. The area of unmanaged forest was set to the total area older than that. If the rotation period had an odd power of ten (50, 70 years etc.), the oldest age class got the sum of the inventoried areas in its starting range up to CCF's range. If the rotation period had an even power of ten (60, 80 years etc.), the second oldest age got 2/3 of the inventoried 20-year area its age was within, and the oldest age class got the remaining area up to CCF's range. This methodology resulted in many cases in a high fraction of forest in the oldest age class, which could result in uneven harvest rates and age-related changes in carbon fluxes between decades. A smoothing of the age-class distribution data was, therefore, done by first reducing the areas with a factor of 2/3 and then add 1/3 of the average area over the rotation period for each species class. When the areas from the 1988-1992 treated this way and then prognosticated and compared to data from the 2018-2022 period there are, however, still quite big discrepancies (Fig. A1).

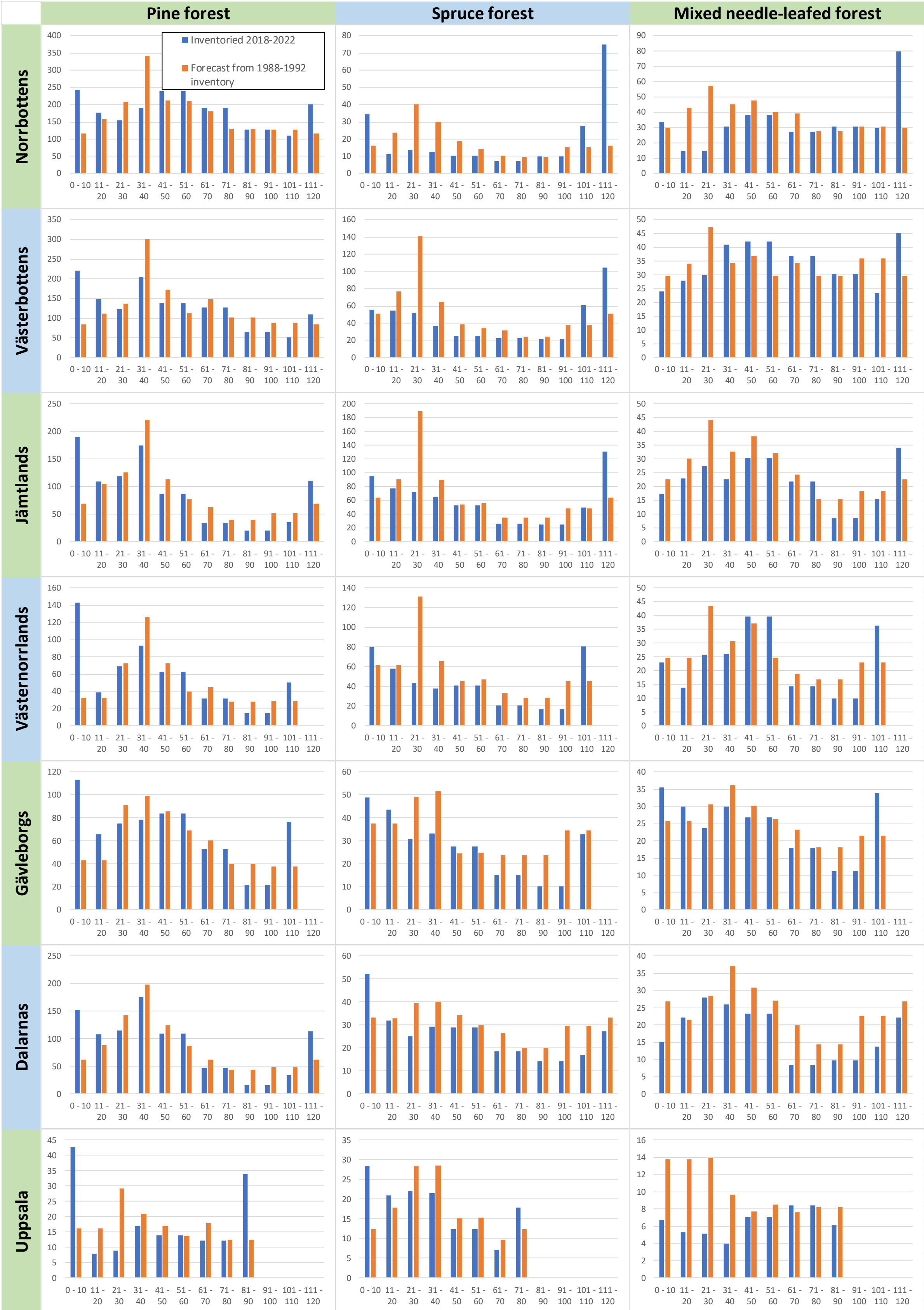

Figure A1. Inventoried data of the forest area (1000 ha) by county from the national forest inventory as transformed to the age and species classes used in the LPJ-GEUSS simulations in year 2020. Data taken directly from the 2018-2022 inventory (blue bars) and prognosticated and smoothed from the 1988-1992 inventory (orange bars).

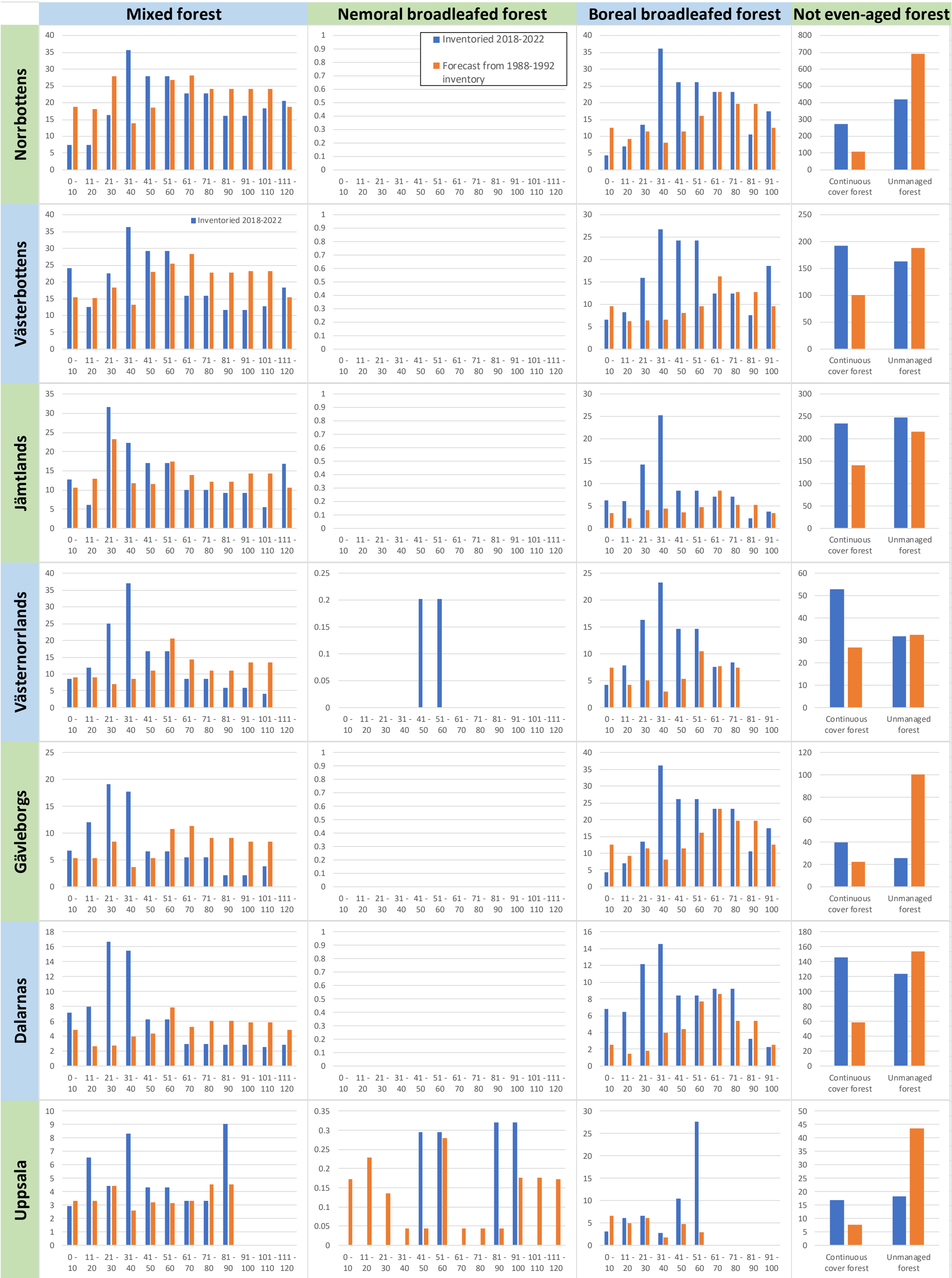

Figure A1. Continued.

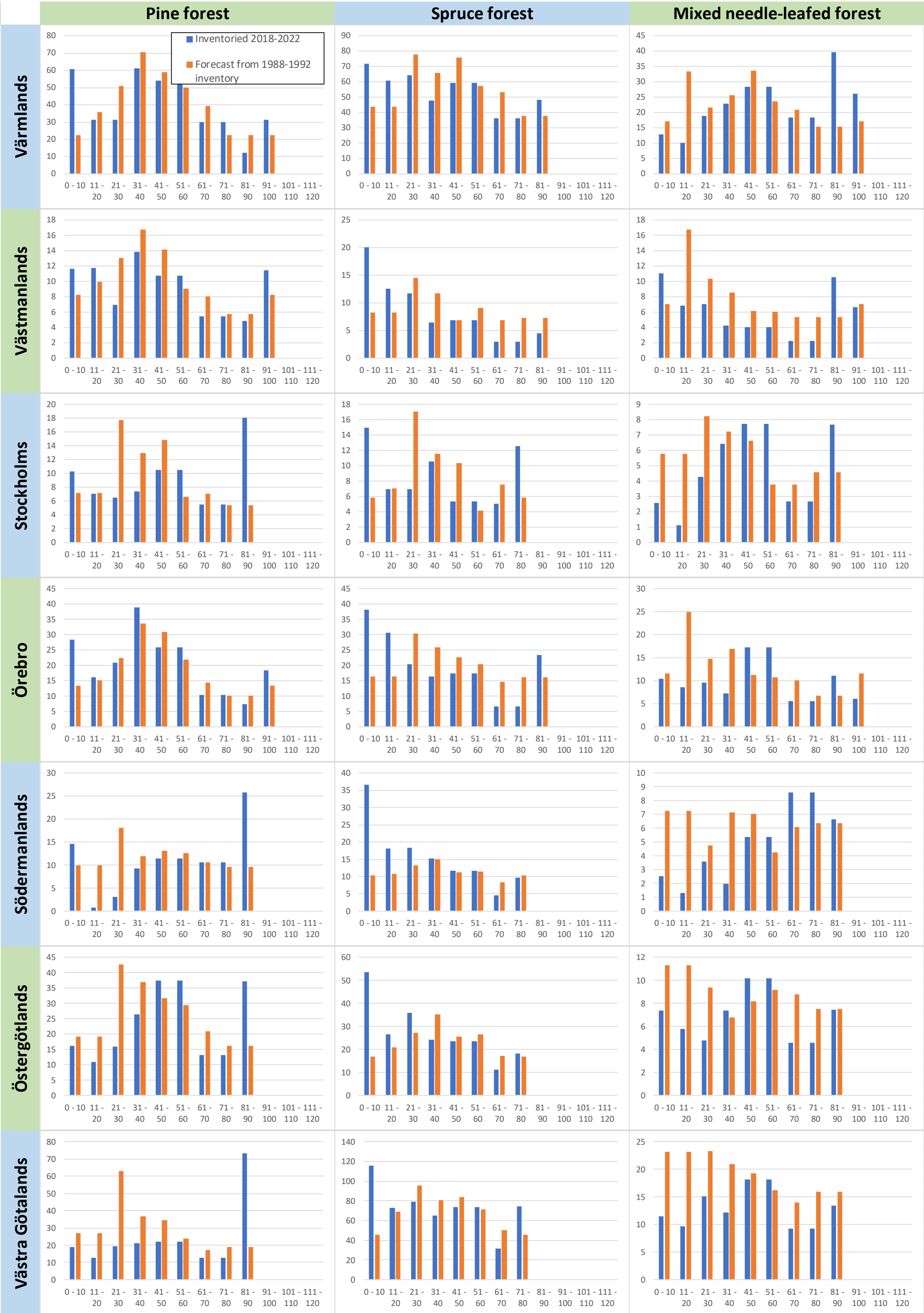

Figure A1. Continued.

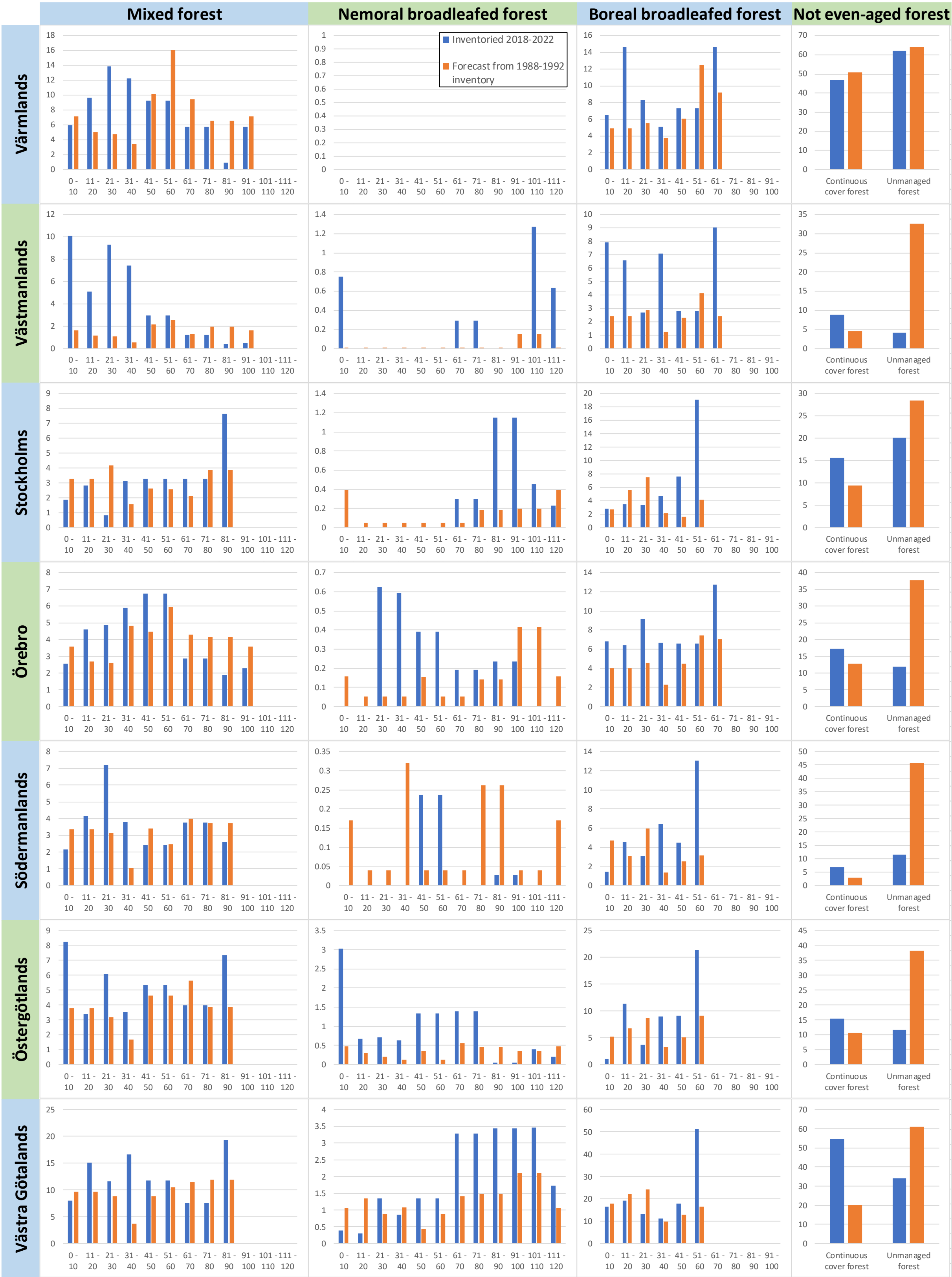

Figure A1. Continued.

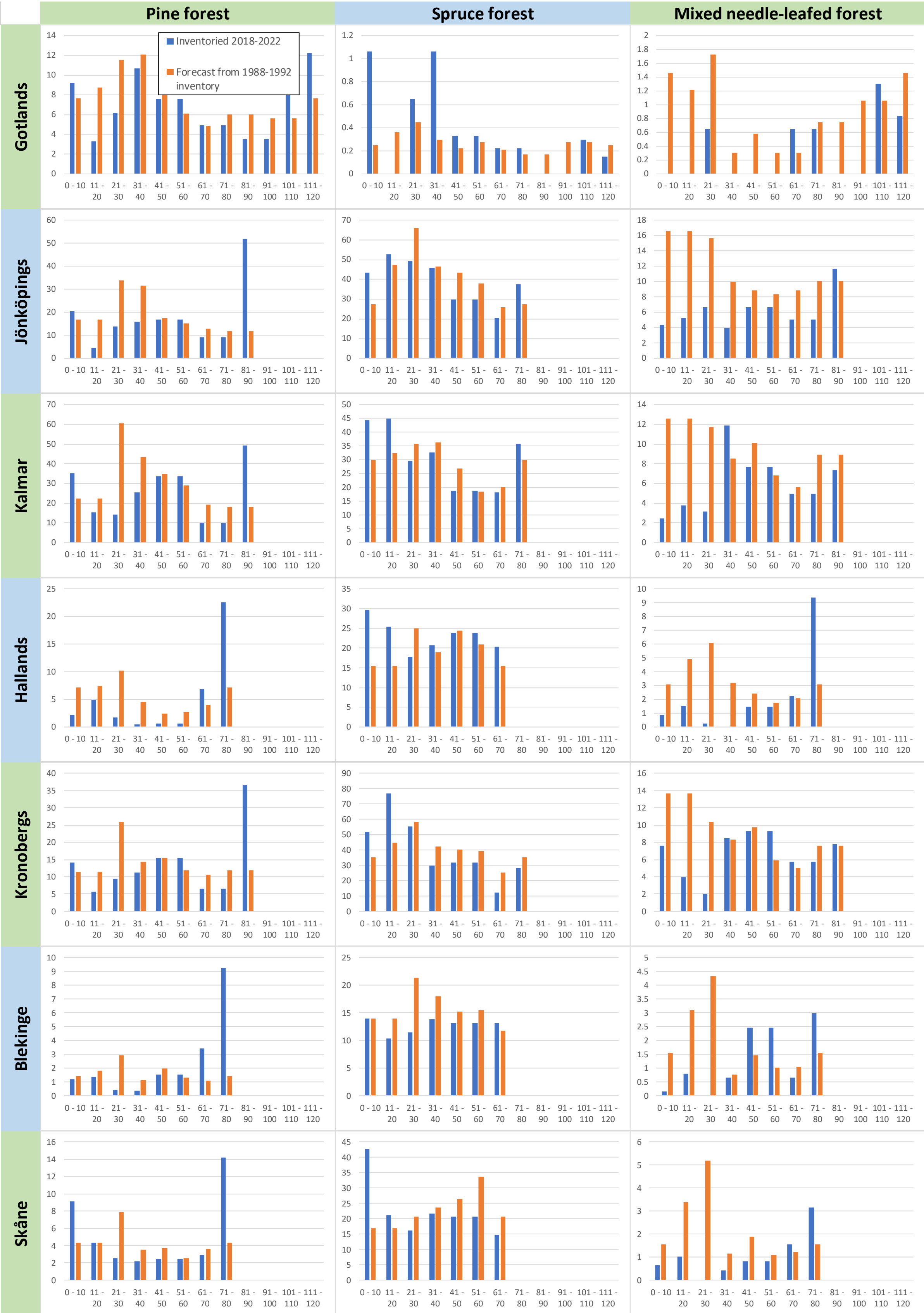

Figure A1. Continued.

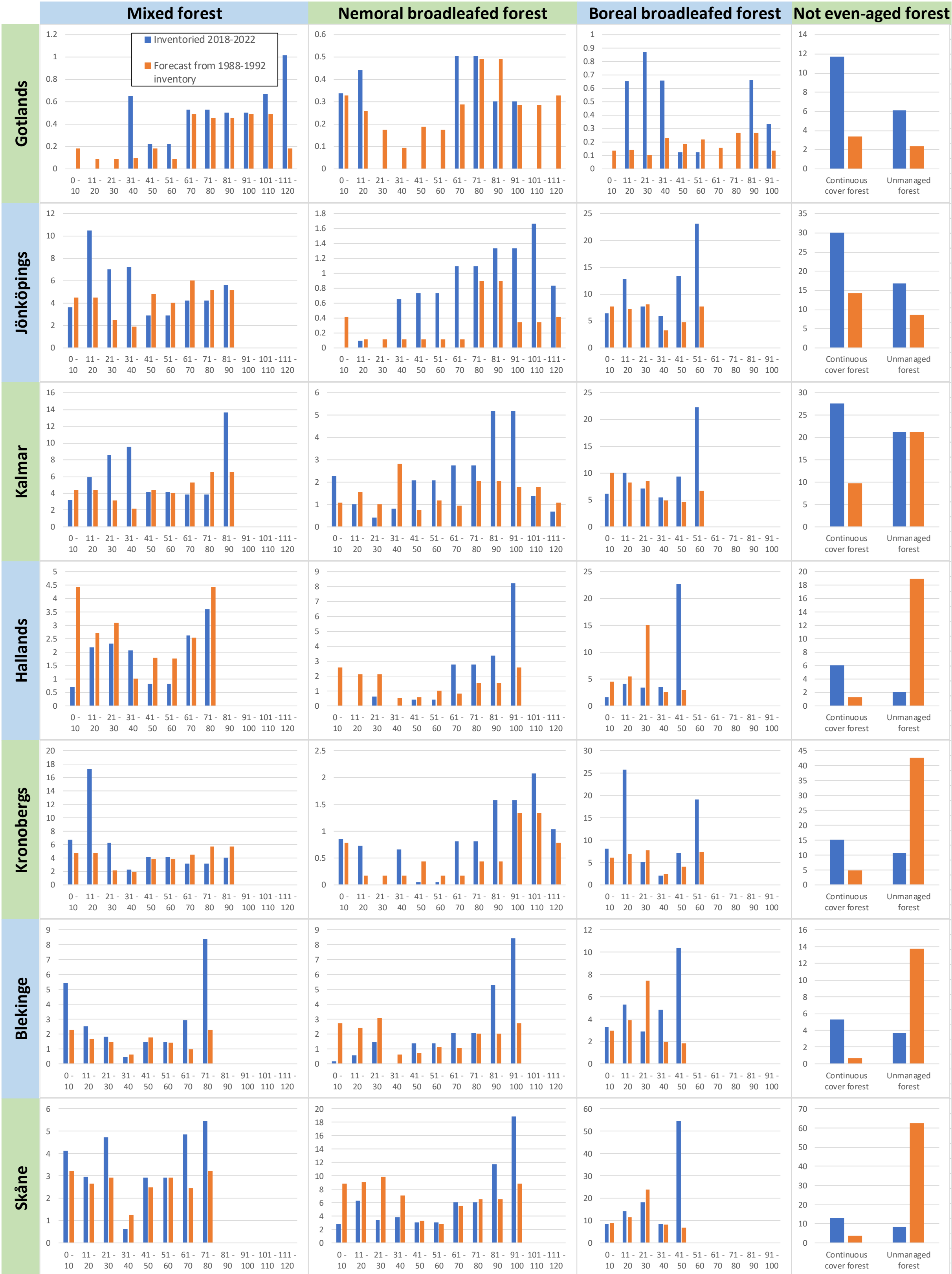

Figure A1. Continued.

To simulate a stand with prescribed age and species type in 1990 with a representative history, a simulated stand was created from potential unmanaged vegetation in the simulation year of one full rotation period plus the prescribed age before 1990 (e.g., a stand that should be 25 years and had a rotation period of 90 years was established in 1875).

In the main run, there was one stand types for each species type and rotation period, where the fractional increase in area over a 10-year period was evenly distributed from the area in the 10-year class. This enabled that each one-year age class was represented in the simulation but simulation outputs were averaged over all age classes within a stand type.

In the complementary run, the stand types were further divided into 10-year classes. Here all the fractional area belonging to a species type and age class was added at once in the centre year. This approach enabled results representing only one age, but a specific age was only simulated for one year in a 10-year period.

The transition of potential natural vegetation to managed stand types was set in a land-use file, specifying the fractional cover of natural and managed forest by year from year 1750 (LUageint.txt and LUfixed.txt for the main and complementary run respectively). And the fractional cover of the different managed stand types by year was similarly provided in forestry files (FORESTageint.txt and FORESTfixed.txt).

The management program with settings for planting and thinning of each stand type is defined in an instruction file. The setting for the clear-cut stand types are summarised in Table A1, and are based on general recommendations (Skogsstyrelsen, 1989ab). For continuous cover forestry the harvest strength was set to 20% of tree biomass removed in each cutting, and the return interval of the cuttings was 20, 18, 16, 14 and 12 years in LPJ-GUESS groups 1-5 respectively.

Table A1. Management setting for the different species types and rotation period groups (Figure 1), defining the number of plants established after clear cut by species, and the age and intensity of thinning. For the pre-commercial thinning (PCT) there was a stronger thinning applied to the cohorts that had naturally regenerated and not been planted.

					Age at pre-commercial thinning (PCT) and thinning					Thinning strength (fraction of biomass removed)					
Forest type	LPJ-GUESS group	Rotation period	Species planted	Plant dens	PCT	Th. 1	Th. 2	Th. 3	Th. 4	PCT-planted	PCT-not planted	Th. 1	Th. 2	Th. 3	Th. 4
Pine	1	120	*Pin_syl*	2000	16	40	72	-	-	0.15	0.9	0.25	0.25	-	-
Pine	2	110	*Pin_syl*	2200	14	36	66	-	-	0.15	0.9	0.25	0.25	-	-
Pine	3	100	*Pin_syl*	2400	12	32	60	-	-	0.15	0.9	0.25	0.25	-	-
Pine	4	90	*Pin_syl*	2600	10	28	54	-	-	0.15	0.9	0.25	0.25	-	-
Pine	5	80	*Pin_syl*	2800	8	24	48	-	-	0.15	0.9	0.25	0.25	-	-
Spruce	1	120	*Pic_abi*	2000	15	35	65	-	-	0.15	0.7	0.25	0.25	-	-
Spruce	2	110	*Pic_abi*	2200	13	32	60	-	-	0.15	0.7	0.25	0.25	-	-
Spruce	3	90	*Pic_abi*	2400	11	27	50	-	-	0.15	0.7	0.25	0.25	-	-
Spruce	4	80	*Pic_abi*	2600	9	24	44	-	-	0.15	0.7	0.25	0.25	-	-
Spruce	5	70	*Pic_abi*	2800	7	21	38	-	-	0.15	0.7	0.25	0.25	-	-
Mixed needle-leafed	1	120	*Pic_abi* *Pin_syl* *Bet_pen*	900 900 200	16	36	72	-	-	0.15	0.9	0.25	0.25	-	-
Mixed needle-leafed	2	110	*Pic_abi* *Pin_syl* *Bet_pen*	990 990 220	14	33	66	-	-	0.15	0.9	0.25	0.25	-	-
Mixed needle-leafed	3	100	*Pic_abi* *Pin_syl* *Bet_pen*	1080 1080 240	12	30	60	-	-	0.15	0.9	0.25	0.25	-	-
Mixed needle-leafed	4	90	*Pic_abi* *Pin_syl* *Bet_pen*	1170 1170 260	10	27	54	-	-	0.15	0.9	0.25	0.25	-	-

Mixed needle-leafed	5	80	*Pic_abi* *Pin_syl* *Bet_pen*	1260 1260 280	8	24	48	-	-	0.15	0.9	0.25	0.25	-	-
Mixed	1	120	*Pic_abi* *Pin_syl* *Bet_pen*	400 600 1000	16	36	72	-	-	0.15	0.9	0.25	0.25	-	-
Mixed	2	110	*Pic_abi* *Pin_syl* *Bet_pen*	440 660 1100	14	33	66	-	-	0.15	0.9	0.25	0.25	-	-
Mixed	3	100	*Pic_abi* *Pin_syl* *Bet_pen*	480 720 1200	12	30	60	-	-	0.15	0.9	0.25	0.25	-	-
Mixed	4	90	*Pic_abi* *Pin_syl* *Bet_pen*	520 780 1300	10	27	54	-	-	0.15	0.9	0.25	0.25	-	-
Mixed	5	80	*Pic_abi* *Pin_syl* *Bet_pen*	560 840 1400	8	24	48	-	-	0.15	0.9	0.25	0.25	-	-

Table A1. Continued.

					Age at pre-commercial thinning (PCT) and thinning					Thinning strength (fraction of biomass removed)					
Forest type	LPJ-GUESS group	Rotation period	Species planted	Plant dens	PCT	Th. 1	Th. 2	Th. 3	Th. 4	PCT-planted	PCT-not planted	Th. 1	Th. 2	Th. 3	Th. 4
Nemoral broad-leafed	1-4	120	*Fag_syl* *Que_rob* *Ulm_gla* *Fra_exc*	800 1200 200 200	10	24	46	68	90	0.2	0.95	0.2	0.2	0.2	0.2
Nemoral broad-leafed	5	100	*Fag_syl* *Que_rob* *Ulm_gla* *Fra_exc*	1000 1500 250 250	7	20	40	60	80	0.2	0.95	0.2	0.2	0.2	0.2
Boreal broad-leafed	1	100	*Bet_pub* *Bet_pen* *Pop_tre*	600 1200 200	15	40	64	-	-	0.15	0.9	0.25	0.25	-	-
Boreal broad-leafed	2	80	*Bet_pub* *Bet_pen* *Pop_tre*	440 1320 440	13	32	52	-	-	0.15	0.9	0.25	0.25	-	-
Boreal broad-leafed	3	70	*Bet_pub* *Bet_pen* *Pop_tre*	240 1440 720	11	28	46	-	-	0.15	0.9	0.25	0.25	-	-
Boreal broad-leafed	4	60	*Bet_pub* *Bet_pen* *Pop_tre*	260 1560 780	9	24	40	-	-	0.15	0.9	0.25	0.25	-	-
Boreal broad-leafed	5	50	*Bet_pub* *Bet_pen* *Pop_tre*	280 1680 840	7	20	34	-	-	0.15	0.9	0.25	0.25	-	-

References

Skogsstyrelsen 1989a. Gallringsmallar Norra Sverige. Tryckeri AB Småland.

Skogsstyrelsen 1989b. Gallringsmallar Södra Sverige. Tryckeri AB Småland.

Simulated forest types

	LPJ-GUESS	ORCHIDEE temperate pft	ORCHIDEE boreal pft
Natural forest	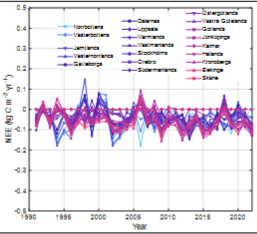		
Pine forest	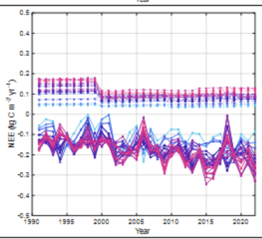		
Spruce forest	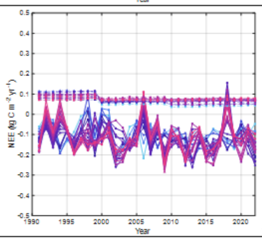	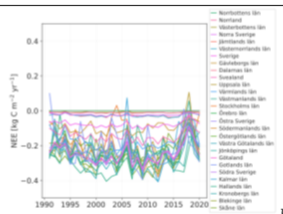	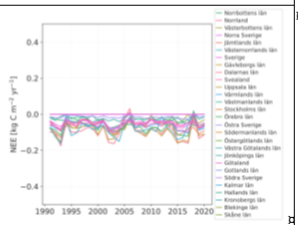
Mixed needle-leafed forest	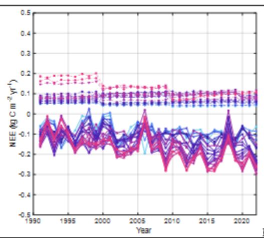	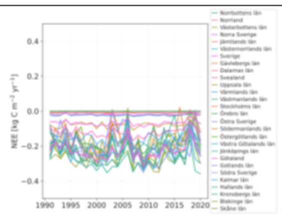	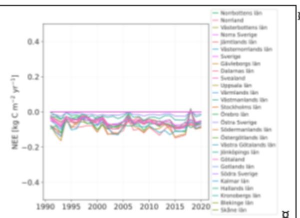
Mixed forest	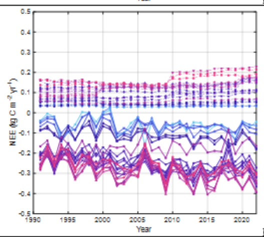		
Nemoral broad-leafed forest	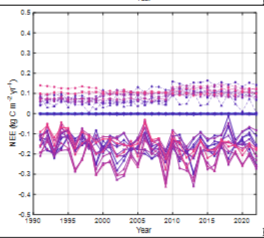	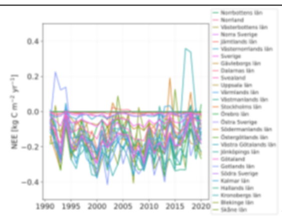	

Figure A2. NEE excluding harvest (solid lines) and carbon removed by harvest (dashed lines) by year 1990-2020 for different forest types. The LPJ-GUESS harvest numbers represent carbon removed from the forest. In ORCHIDEE, harvested wood enters soft, medium or hard wood pools and emissions are subsequently calculated for these separate pools and not for each PFT separately.

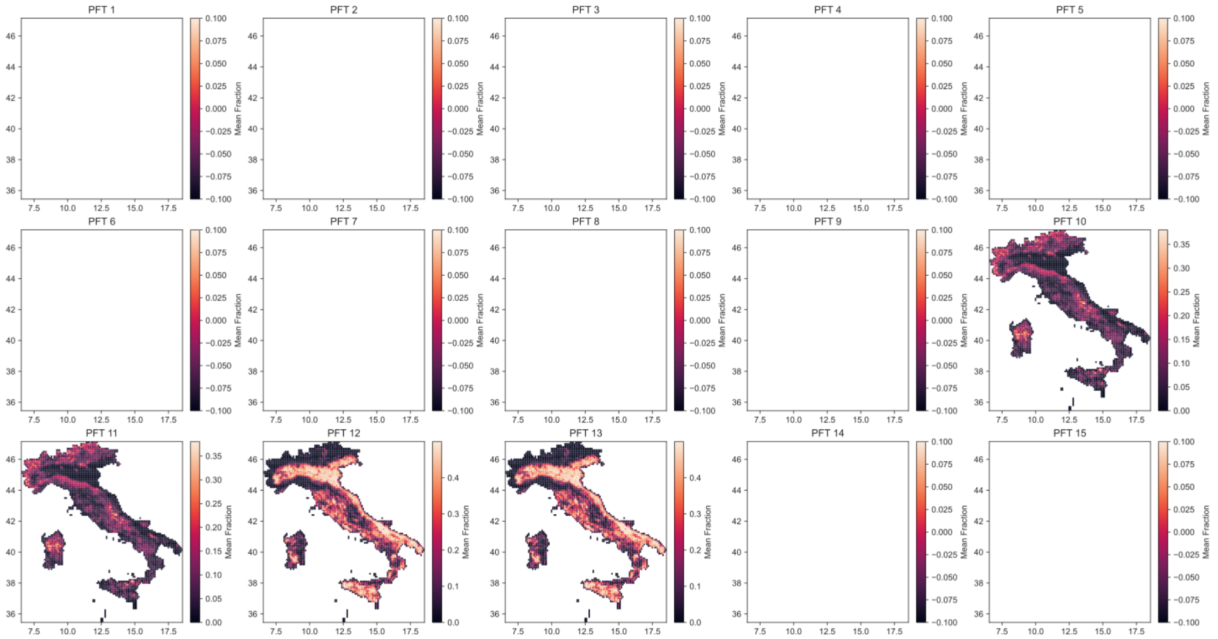

Figure X. The land cover fractions of crops (PFT 12 and PFT 13) and grasses PFT 10 and PFT 11 used in the Itay case-study with ISPRA input.

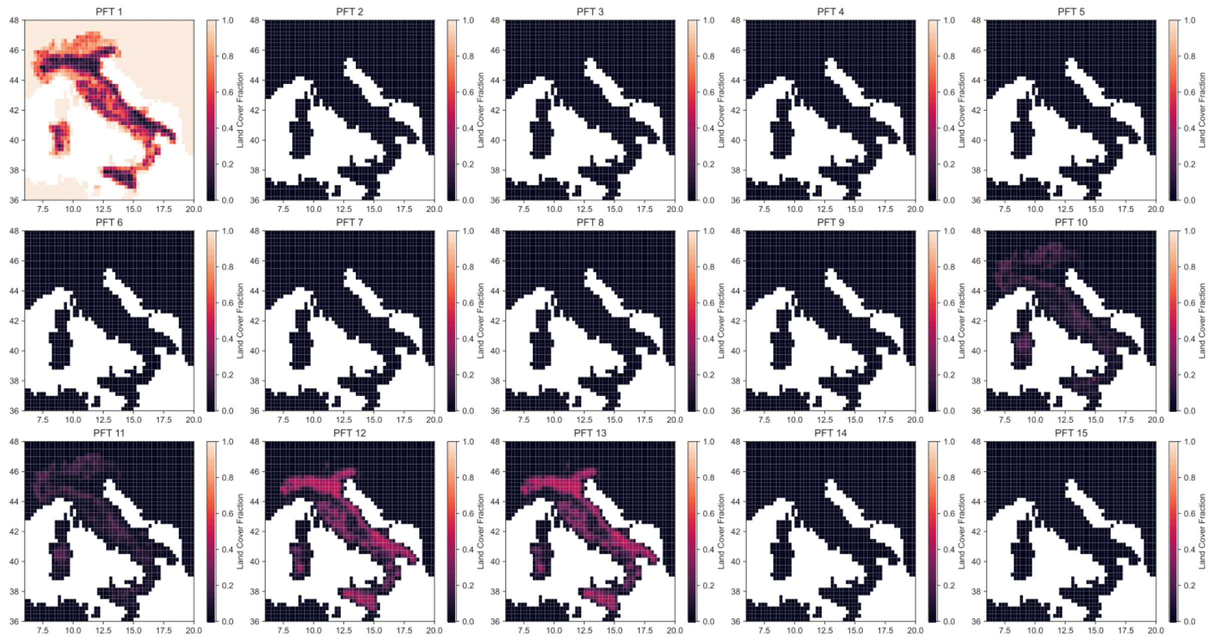

Figure A4. The land cover fractions of crops (PFT 12 and PFT 13) and grasses PFT 10 and PFT 11 and bare ground (PFT 1) used in the Itay case-study with ISPRA input.

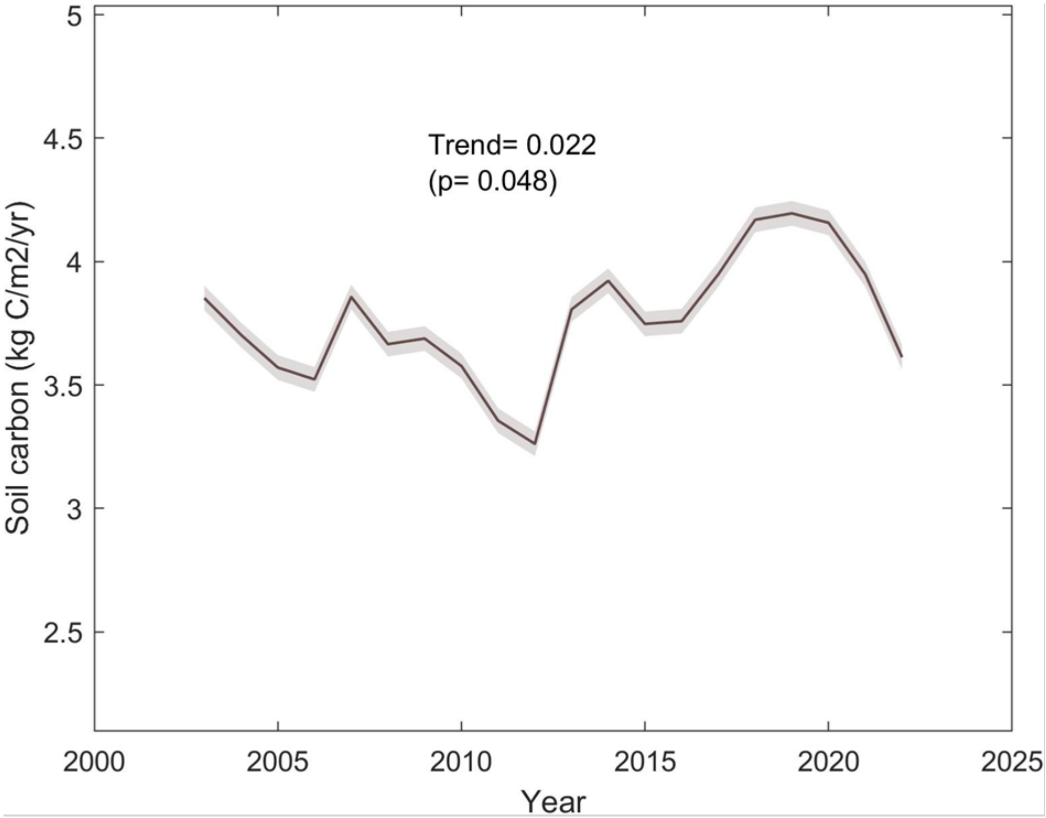

Figure A5. Time series of soil carbon stocks for Swedish forests based on Swedish National Forest Inventories over the period 2003 – 2022.